Jasmonate Perception by Inositol-phosphate-potentiated COI1-JAZ Co-receptor

Laura B. Sheard

A dissertation submitted in partial fulfillment of the
requirements for the degree of

Doctor of Philosophy

University of Washington

2012

Program Authorized to Offer Degree:
Pharmacology

University of Washington
Graduate School

This is to certify that I have examined this copy of a doctoral dissertation by

Laura B. Sheard

and have found that it is complete and satisfactory in all respects
and that any and all revisions required by the final
examining committee have been made.

Chair of the Supervisory Committee:

_____
Ning Zheng

Reading Committee:

_____
Ning Zheng

_____
Chris Hague

_____
Richard Gardner

Date: _____

In presenting this dissertation in partial fulfillment of the requirements for the doctoral degree at the University of Washington, I agree that the Library shall make its copies freely available for inspection. I further agree that extensive copying of the dissertation is allowable only for scholarly purposes, consistent with "fair use" as prescribed in the U.S. Copyright Law. Requests for copying or reproduction of this dissertation may be referred to Proquest Information and Learning, 300 North Zeeb Road, Ann Arbor, MI 48106-1346, 1-800-521-0600, to whom the author has granted "the right to reproduce and sell (a) copies of the manuscript in microform and/or (b) printed copies of the manuscript made from microform."

Signature _____

Date _____

University of Washington

Abstract

Jasmonate Perception by Inositol-phosphate-potentiated COI1-JAZ Co-receptor

Laura B. Sheard

Chair of the Supervisory Committee:
Professor Ning Zheng
Department of Pharmacology

Jasmonates (JAs) are a family of plant hormones that regulate plant growth, development, and responses to stress. The F-box protein CORONATINE-INSENSITIVE 1 (COI1) mediates JA signaling by promoting hormone-dependent ubiquitination and degradation of transcriptional repressor JAZ proteins. Despite its importance, the mechanism of JA perception remains unclear. Here we present structural and pharmacological data to show that the true JA receptor is a complex of both COI1 and JAZ. COI1 contains an open pocket that recognizes the bioactive hormone, (3*R*,7*S*)-jasmonoyl-L-isoleucine (JA-Ile), with high specificity. High-affinity hormone binding requires a bipartite JAZ degron sequence consisting of a conserved a-helix for COI1 docking and a loop region to trap the hormone in its binding pocket. In addition, we identify a third critical component of the JA co-receptor complex, inositol

pentakisphosphate, which interacts with both COI1 and JAZ adjacent to the ligand. Our results unravel the mechanism of JA perception and highlight the ability of F-box proteins to evolve as multi-component signaling hubs.

TABLE OF CONTENTS

LIST OF FIGURES

LIST OF TABLES

ACKNOWLEDGEMENTS

This work would not have been possible without the help from all members of the Zheng Laboratory and the generous support from the Cellular and Molecular Biology Training Grant from National Institutes of Health, T32 GM07270.

DEDICATION

For My Family

CHAPTER 1

Introduction to plant hormones and their receptors

For much of the Kingdom Plantae, life and developmental choices are regulated almost exclusively by a handful of small organic molecules, the phytohormones. Many of these hormones are produced locally in the plant and transported to target tissues within the plant either from cell to cell transport or through the vasculature. Other hormones are volatilized and are sensed by distal portions of the same plant, or by other nearby plants. The first five "classic phytohormones" identified were auxin, gibberellin, cytokinin, ethylene, and abscisic acid. Since then, a number of other hormones have been isolated, including salicylic acid, jasmonates, brassinosteroids, and strigolactones.

The receptors for phytohormones are diverse. Ethylene and cytokinins are sensed by transmembrane receptors, which resemble the two-component systems in prokaryotes. Brassinosteroids activate their signal transduction cascades through leucine-rich repeat receptor kinases (LRR-RKs), which are also transmembrane proteins commonly utilized by other eukaryotes including mammals. Recent studies have shown that auxin, jasmonate, gibberellin, and possibly strigolactones signal through a unique and novel signal transduction mechanism. The direct target of these hormones is the Skp1-Cul1-F-box protein (SCF) family of E3-ubiquitin ligases, which catalyze ubiquitination and degradation of their polypeptide substrates. In addition, the receptors for

abscisic acid have also been identified recently. Here I will summarize the process in receptor identification and characterization for select plant hormones.

1.1 Auxin and TIR1

In 1880, twenty years after the publication of *On the Origin of Species* and two years before he passed away, Charles Darwin, together with his son Francis, published a less well-known book, entitled *The Power of Movements in Plants*. The studies they described in this book initiated more than one century long investigations of an important small molecule, auxin, the first plant hormone ever identified. By tracking the slow movements of plants during growth and under external stimuli, Darwin analyzed plant phototropism in details. He noted that the coleoptile, an ensheathing organ of the grass seedlings, would normally bend toward a light source, unless the tip of the plant was either removed or covered by a light proof cap. Darwin concluded "that with some seedling plants the uppermost part alone is sensitive to light, and transmits an influence to the lower part, causing it to bend." Without knowing the nature of this "influence", he further postulated that the phototropic bending of the plant might be caused by "increased turgescence of the cells" (cell elongation) on one side of the plant "followed by increased growth", all in response to the "influence" sent from the plant tip.

The "influence" proposed by Darwin was isolated, more than four decades later, by Fritz Went in his graduate studies. By allowing the "influence" to diffuse from grass coleoptile tips to agar blocks and showing that the latter

could replace the former to promote plant growth, Fritz Went demonstrated that this "influence" is a diffusible substance that was transported from the plant tip to the subjacent tissues. In his experiments, when the agar block was placed right on top of a decapitated grass coleoptile, the plant grew straight up. But when the agar block was shifted off-center, it would induce curved growth of the plant in the dark, mimicking the bending of the plant toward light. Phototropism, therefore, can be explained by the higher concentration of the diffusible matter sent from the tip to the shade side of the plant, which leads to asymmetrical growth and bending of the plant (Fig. 1.1). Fritz Went proposed that this diffusible matter was a plant hormone, which was later named auxin. The term comes from the Greek word "auxein", which means "to grow".

Chemically identified as indole-3-acetic acid, auxin has since been studied extensively and characterized as the most potent growth-regulating plant hormone (Woodward and Bartel, 2005). A number of natural and synthetic auxin analogues have been found. Although they have rather distinct chemical structures, all can induce auxin responses in plants and are often collectively referred to as auxins. A myriad of studies have shown that auxin regulates a wide range of growth processes throughout plant development. These include, but are not limited to, embryogenesis, root and shoot development, tropic responses to light and gravity, vascular differentiation, apical dominance, as well as flower and fruit development. A good example illustrating the important role of auxin in plant growth is the auxin-dependent maturation of strawberries. During development, strawberry seeds produce auxin to promote the growth of

the fruit. When the seeds are removed (easy to do since they are on the surface of the fruit), the development of strawberries stops. Remarkably, artificially applied auxin alone is sufficient to restore the normal maturation of the fruit without the seeds. Just like most biological hormones, excess amount of auxin is harmful to many plants. 2,4-D (2,4-dichlorophenoxy acetic acid) is a synthetic auxin widely used as a weed killer. It is also one of the active ingredients of "agent orange" used by the U.S. military to defoliate the forest in Vietnam during the Vietnam War.

Auxin not only regulates the division, elongation, and differentiation of individual cells, but also functions as signals between cells, tissues, and organs, contributing to the coordination of growth in the whole plant. While many mechanistic details remain to be revealed, it is well recognized that plants generate asymmetric accumulation of auxin in their bodies in response to developmental and environmental cues (Woodward and Bartel, 2005). The resulting auxin gradients vary dramatically throughout the body and life of the plant. A highly complex network of pathways regulating auxin synthesis, degradation, and conjugation, together with intercellular polar auxin transport systems, is responsible of spatially and temporally modulating the cellular auxin levels.

Despite the extensive studies on auxin homeostasis, a central question about auxin action remains unanswered: how is auxin perceived by the plant cells? Related to this, how is the auxin signal translated into the physiological responses? Early efforts to identify auxin receptors focused on isolating proteins

that show high affinity to auxin. This straightforward biochemical approach led to the discovery of a single protein named auxin-binding protein 1 (ABP1), which is mainly localized to the endoplasmic reticulum (Henderson et al., 1997). Although subsequent studies have implicated ABP1 in cell elongation and embryonic development, auxin-dependent cell division still occurs in the absence of the protein. Therefore, the role of ABP1 as a central auxin sensor remains controversial. Importantly, the function of ABP1 has little connection to gene activation, which has long been associated with auxin response. An auxin sensor is anticipated to function upstream of a signaling pathway leading to transcriptional control.

Thanks to the molecular biology approach, such an auxin response pathway has been indeed elucidated based on the identification of the transcripts showing auxin-induced accumulation (Fig. 1.1). Analyses of the promoter regions of the genes encoding these early and primary auxin-induced transcripts helped reveal a common DNA sequence, known as the Auxin-Response Element, or AuxRE (Ulmasov et al., 1995). The identification of the AuxRE soon led to the discovery of a family of transcription factors, called Auxin Response Factors, or ARFs (Liscum and Reed, 2002; Ulmasov et al., 1997). With a domain capable of binding to the AuxRE DNA sequence, many of these ARF transcription factors function as transcriptional activators. Interestingly, a major family of auxin response genes that are regulated by ARFs, named *Aux/IAAs,* encode protein products that act as the repressors of the ARF transcription factors. Upon directly binding to the ARF proteins, the Aux/IAA

proteins can repress gene transcriptions, thereby, providing a negative feedback mechanism for the auxin responses (Fig. 1.1). Evidently, finding out how auxin regulates Aux/IAAs might help elucidate how auxin is sensed and how auxin signaling works.

Forward genetic screens of auxin resistant mutants in Arabidopsis led to the major breakthroughs in unraveling the regulators of Aux/IAAs. While some of the mutants identified in these screens carry gain-of-function mutations of the *Aux/IAA* genes themselves, the rest of the auxin resistant mutants all point to enzymes of the ubiquitin-dependent proteolytic pathway. It was soon recognized that Aux/IAAs are tightly regulated by ubiquitination and protein turnover.

Ubiquitin-dependent proteolysis has emerged in recent years as a universal protein regulatory mechanism that is widely used by eukaryotes. By altering the turnover of a target protein, a pathway can be either up-regulated or down-regulated, depending on whether the target is an inhibitor or activator. To selectively degrade a protein substrate, eukaryotic cells label the substrate with a polyubiquitin chain, which serves as a targeting signal for the proteasome. An E1-E2-E3 three-enzyme cascade mediates protein modification by ubiquitin. In this cascade, the E3 ubiquitin ligase plays a central role as it not only catalyzes the attachment of ubiquitin to the substrate, but also determines the specificity of the reaction. Whereas the human genome contains only one ubiquitin E1 and 20-30 E2 enzymes, the number of E3s is estimated to reach almost one thousand. This number is even higher in plants.

Intriguingly, several auxin resistant mutants identified by genetic screens have defects in the subunits of a cellular ubiquitin ligase machinery, SCF, and its regulatory factors (Dharmasiri and Estelle, 2004). As one of the best-studied multi-subunit ubiquitin ligases in eukaryotes, the SCF complex consists of three basal protein components and an interchangeable subunit, which are Cul1, Rbx1, Skp1 (ASK1 in plants), and the F-box protein. Cul1-Rbx1 forms the catalytic core of the complex, while Skp1 serves as an adaptor, responsible of docking different F-box proteins to the E3 complex. The F-box proteins, bearing an Skp1-interacting F-box motif and a protein-protein interaction domain, in turn recruit different protein substrates to the SCF. One of the auxin resistant mutants, TIR1, encodes a plant F-box protein, implicating that the SCF-TIR1 complex is a crucial player in the auxin signaling pathway (Gray et al., 1999; Gray et al., 2001). Given that wild type Aux/IAA proteins generally have a high turnover rate and that the auxin-resistant gain-of-function mutations of *Aux/IAAs* confer unusual stability to the gene products, it was readily appreciated that the substrates of SCF-TIR1 are in fact the Aux/IAA transcription repressors. Gene activation in response to auxin, therefore, is achieved through SCF-TIR1-mediated ubiquitination and proteasome-degradation of Aux/IAAs.

The SCF ubiquitin ligases have been well studied in both budding yeast and human cells. In all known cases, SCF-mediated protein ubiquitination is tightly regulated by cellular signaling. The substrates of the SCF are almost always phosphorylated in response to cellular cues before they can be recognized by the F-box proteins. This requirement ensures that the substrate degradation by

the SCF is temporally and differentially controlled. How then does auxin regulate the recognition of Aux/IAAs by SCF-TIR1 for ubiquitination? Is there an upstream auxin sensor, which, upon binding to auxin, triggers the phosphorylation of Aux/IAAs? Surprisingly, the turnover of Aux/IAAs is independent of any phosphorylatable residue. In response to auxin, no stable modification of the Aux/IAA proteins in any form was found.

The century-long quest of auxin action in plants reached a milestone in 2005 when two groups simultaneously reported that SCF-TIR1 itself actually functions as a direct auxin receptor. Using an affinity pull down assay, Mark Estelle's group and Ottaline Leyser's group both showed that, in an auxin and dose dependent manner, bacteria-produced GST-Aux/IAA7 or a biotinylated Aux/IAA7 peptide was able to co-precipitate TIR1, which was synthesized in two metazoan systems (Dharmasiri et al., 2005; Kepinski and Leyser, 2005). Furthermore, the TIR1-IAA complex could specifically pull down radiolabelled auxin. Since no other plant proteins could possibly exist in these assays, the TIR1 and/or IAA proteins must directly interact with auxin, serving as the long sought receptor (Fig. 1.1). Together with many previously studies, these reports finally provide a satisfying molecular description of the complete signal transduction cascade of auxin signaling, which at least partially explains the plant phototropic behavior observed and studied by Charles Darwin and Fritz Went. Upon exposure to light, the tip of grass coleoptile produces auxin, which is uni-directionally transported and accumulated to the side of the plant in shade. The increased concentration of auxin in the target cells is "sensed" by SCF-

TIR1, whose ubiquitination activity toward Aux/IAAs becomes greatly enhanced. The accelerated ubiqutination of Aux/IAAs leads to their rapid degradation, thereby releasing the ARFs that are otherwise repressed. Finally, the resulting free ARFs activate directly or indirectly the transcription of genes responsible of promoting cell growth.

In spring of 2007, the Zheng laboratory published crystal structures of the ASK1-TIR1 complexes with auxin and Aux/IAA degron peptides bound (Tan et al., 2007). The structures showed that upon binding to TIR1, auxin fills a gap between the F-box protein and the substrate degron peptide, acting like a "molecular glue" to enhance their affinity for one another. It is notable that substrate binding did not allosterically modulate substrate binding, but directly altered the landscape of the binding pocket to increase the binding of Aux/IAA to promote TIR1-catalyzed ubiquitination. Because the Aux/IAA degron peptide essentially encloses auxin in the TIR1 pocket, it raises the possibility that the true receptor of the hormone is a co-receptor system, which consists of both the F-box protein and its substrate polypeptide. Quantitive ligand binding studies, however, are essential to prove this hypothesis.

By serendipity, the crystal structure also revealed an unexpected inositol hexakisphosphate ($InsP_6$) molecule, which was co-purified with TIR1 and located in the center of the TIR1 LRR domain underneath the auxin-binding pocket. In the crystal, the $InsP_6$ molecule is surrounded by more than 10 positively charged residues, most of which are strictly conserved in known plant TIR1 orthologues. This surprising finding strongly suggested that $InsP_6$ might

function as a critical co-factor of the TIR1 F-box protein, although further evidence is needed to validate its role in the auxin receptor.

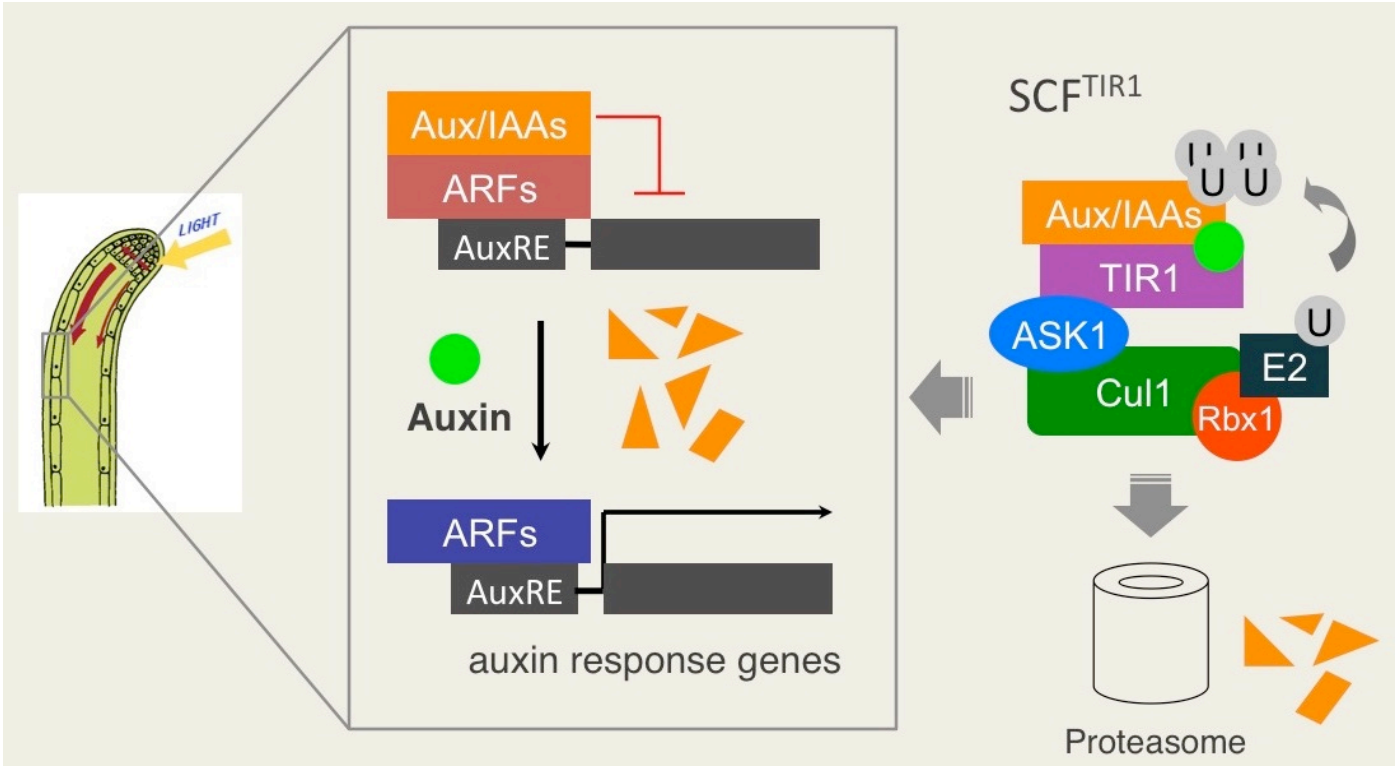
LIGHT
Aux/IAAs
ARFs
AuxRE
Auxin
ARFs
AuxRE
auxin response genes
SCF^TIR1
U
U
U
Aux/IAAs
TIR1
ASK1
Cul1
E2
Rbx1
Proteasome

Fig.1.1 The auxin signaling pathway. Upon sensing lateral light, auxin is transported and accumulated along the side of the plant in shade. In the presence of auxin, the transcription of auxin response genes is turned on due to SCF-TIR1-mediated degradation of Aux/IAAs, which are transcription repressors that inhibit the action of the transcription activator ARFs. Auxin binds directly to the substrate receptor subunit of SCF-TIR1, the TIR1 F-box protein, which is responsible for recruiting Aux/IAAs to the E3 complex.

1.2 Abscisic acid and PYR/PYL/RCAR

To survive and flourish in rapidly changing environmental conditions, plants use a complex family of hormones to regulate growth and reproduction. One plant hormone, abscisic acid (ABA), coordinates responses to stressors such as drought, extreme temperature and high salinity, as well as regulating non-stress responses including seed maturation and bud dormancy. Because of its essential function in plant physiology, targeting the ABA signalling pathway holds enormous promise for future application in agriculture.

Identification of the ABA receptor has been unusually challenging. Since 2006, several proteins have been suggested as possible ABA receptors, but their exact roles in ABA signalling remained controversial. In May 2009, a new family of proteins was reported as candidate ABA sensors (Ma et al., 2009; Park et al., 2009). Members of this family, known as PYR/PYL/RCAR proteins, were found to bind ABA and inhibit the activity of specific protein phosphatase enzymes, the type 2C plant PP2Cs, which were previously implicated in the ABA response. In 2010, six independent groups simultaneously defined the structural and functional mechanisms by which ABA is sensed by this newly identified protein receptor (Fujii et al., 2009; Melcher et al., 2009; Miyazono et al., 2009; Nishimura et al., 2009; Santiago et al., 2009; Yin et al., 2009).

The elegant reconstitution assays have been reported that pinpoint the minimal pathway sufficient to recapitulate ABA signalling in plant protoplasts (cells with their cell wall removed) and *in vitro*, tying together the receptor, phosphatase and downstream kinase signalling components. Phosphatases and

kinases exert opposite regulatory effects by respectively removing and adding phosphate groups to substrate proteins. As described in Figure 1.2, in the absence of ABA, the phosphatase PP2C acts as a constitutive negative regulator of a family of kinases (SnRK2) whose autophosphorylation is required for kinase activity towards downstream targets. When ABA binds, it enables the PYR/PYL/RCAR receptor to subsequently bind to and repress PP2C. Sequestration of PP2C permits auto-activation of the kinase, which phosphorylates downstream transcription factors and facilitates transcription of ABA-responsive genes. This pathway is attractive in its simplicity and offers a seamless complement to the known body of ABA literature.

The crucial step in this pathway is perception of ABA by the PYR/PYL/RCAR proteins and the inhibition of PP2C by the ligand (ABA)-bound receptor. Five crystallographic studies have converged to paint a complete picture of these events. Together, they reveal the atomic structures of several PYR/PYL/RCAR proteins in different functional states. Studies, in particular, have captured the structures of PYL2 in all critically relevant forms (ligand-free, ligand-bound and ligand/phosphatase-bound), and allow detailed analyses of the conformational changes that PYL2 undergoes on binding first to the hormone, and subsequently to the phosphatase.

The first highlight of these studies is the ligand-binding mechanism, which is regulated by the opening and closing of a gating loop on the ABA-binding pocket. In the absence of the hormone, the PYR/PYL/RCAR proteins present an open and accessible cavity. Two flexible surface loops, together with

several nearby structural elements, guard the entrance of the cavity. When this water-filled pocket is occupied by ABA, one of the loops closes like a gate, approaching the other loop and sequestering ABA within the pocket (Fig. 1.2). Because most of the amino-acid residues in contact with ABA, as well as the sequences of the two entrance loops, are evolutionarily conserved among all PYR/PYL/RCAR proteins, the ABA-binding and open-to-close gating mechanisms are likely to be common for all members of the receptor family.

Three of the five groups extend their crystallographic studies to describe the architecture of the complex formed between an ABA-bound receptor and PP2C. These structures reveal that the ABA-bound receptors dock onto PP2Cs through a large complementary interface that involves the active site of the phosphatase and the two entrance loops of the receptor. A conserved tryptophan residue of the phosphatase inserts its side chain next to the gating loop, locking it closed. In turn, the gating loop interacts closely with the substrate-binding and active site of the phosphatase, blocking its ability to bind and dephosphorylate its substrate. Together, these structural features comprehensively explain how the PYR/PYL/RCAR proteins inhibit PP2C activity in an ABA-dependent manner, and how PP2Cs act as a potent co-receptor to enhance the affinity of the hormone for its receptor.

These reports present us with a consistent view of ABA signalling that also raises questions for future work. In three of the structural studies, receptor dimerization is observed in the absence of PP2C; and although it is not discussed in the text, dimerization is also present in structural models of the remaining two

studies. But the exact purpose of receptor dimerization remains unclear. In the structure of homodimeric PYR1, only one molecule of ABA can bind per dimer, whereas in the related structure of PYL homodimers, both subunits are occupied. In all of the structural models, the dimer interface involves the flexible gating loop of the receptor, suggesting that dimerization may be functionally relevant. However, receptor dimerization is clearly not required for the final action of the hormone, because only monomeric ABA-bound receptor is found in complex with PP2C.

The movement of the gating loop in PYR/PYL/RCARs to create a hormone-dependent PP2C-binding site is reminiscent of the 'closing lid' mechanism used by the receptor GID1 to sense gibberellin. In this case, hormone binding induces a movement of parts of GID1 that cover the hormone-binding pocket, creating a site for GID1 to bind to substrate proteins and initiate another form of chemical modification, ubiquitylation (Murase et al., 2008; Shimada et al., 2008). Both ABA and gibberellin allosterically remodel their respective receptors, in contrast to the 'molecular glue' mechanism used by auxin (Tan et al., 2007). Although the precise mechanistic details may differ, there is a common feature in plant hormone action at soluble receptors: the hormone signal enhances protein–protein interactions to modulate critical modifications — either phosphorylation or ubiquitylation — that will alter the activity of the target protein. In addition, in all cases, the hormone binds to a site that is directly at or near the protein–protein interface, engaging the associating protein as a co-receptor.

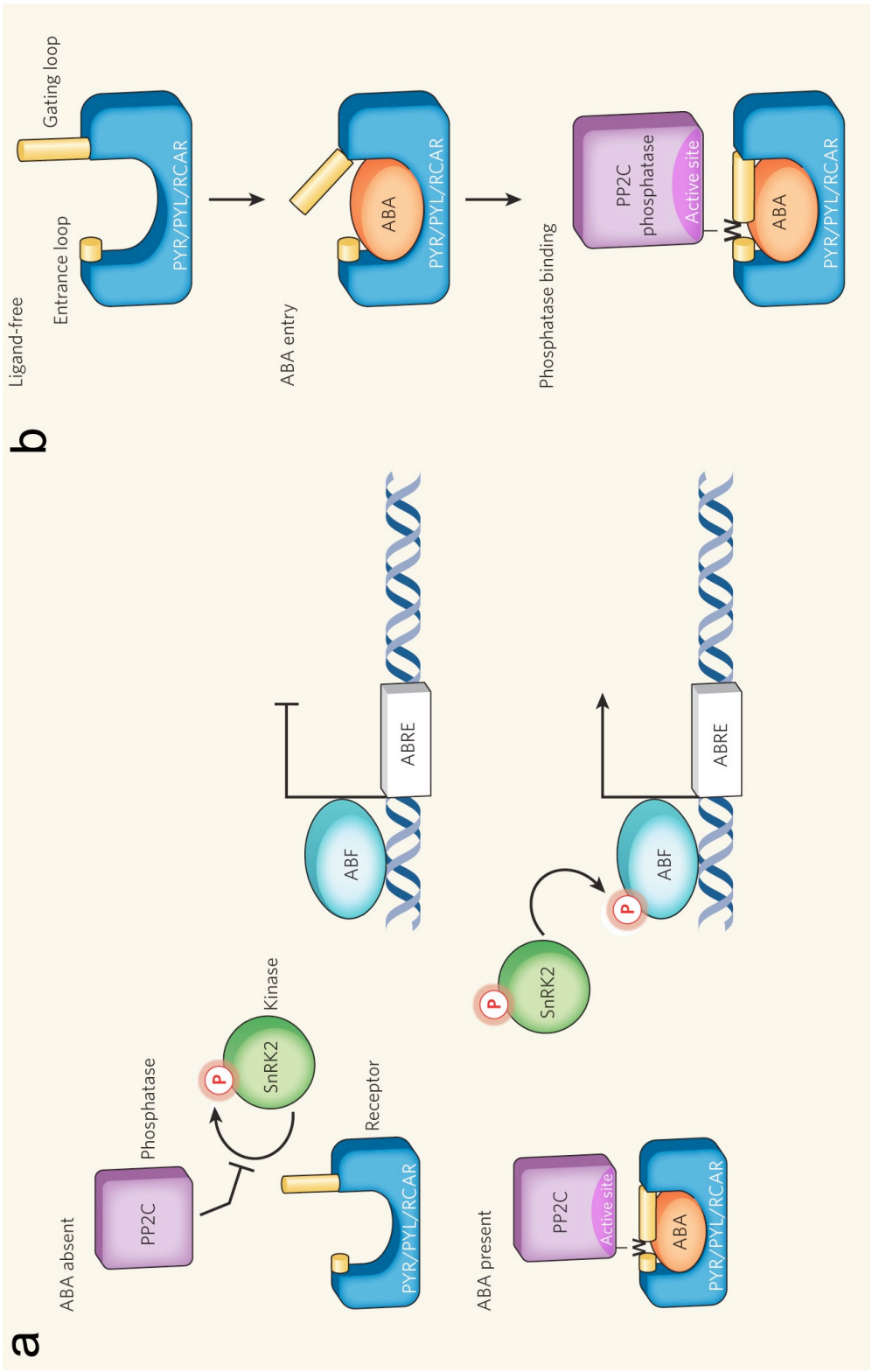
a
ABA absent
PP2C
Phosphatase
P
SnRK2
Kinase
Receptor
PYR/PYL/RCAR
ABF
ABRE
ABA present
PP2C
Active site
ABA
PYR/PYL/RCAR
SnRK2
P
ABF
ABRE
b
Ligand-free
Gating loop
Entrance loop
PYR/PYL/RCAR
ABA entry
ABA
PYR/PYL/RCAR
Phosphatase binding
PP2C
phosphatase
Active site
ABA
PYR/PYL/RCAR

Figure 1.2 Minimal abscisis acid (ABA) signalling pathway and the structural mechanism of ABA action. Left. In the absence of the plant hormone ABA, the phosphatase PP2C is free to inhibit autophosphorylation of a family of SnRK kinases. ABA enables the PYR/PYL/RCAR family of proteins to bind to and sequester PP2C. This relieves inhibition on the kinase, which becomes auto-activated and can subsequently phosphorylate and activate downstream transcription factors (ABF) to initiate transcription at ABA-responsive promoter elements (ABREs). Right, in the ligand-free form, the ABA receptor PYR/PYL/RCAR presents an open and accessible cavity with two flexible surface loops that guard the cavity's entrance. ABA initiates an allosteric open-to-close transition of the gating loop, allowing it to approach the second entrance loop and sequester ABA in the pocket. This exposes a hydrophobic binding site on the gating loop. The phosphatase PP2C binds to the hydrophobic site on the gating loop, inserting a conserved tryptophan (W) next to the gating loop and locking it closed. In turn, the gating loop interacts closely with the active site of the phosphatase, blocking its ability to bind to its substrate.

1.3 Strigolactones and MAX2

Viewed as the most damaging of any agricultural pest, obligate hemiparasitic plants from the broomrape family such as *Striga spp*. and *Orobanche spp*. are the scourge of developing and third-world nations struggling to produce cereal and other crops. These parasitic plants are obligate biotrophs, plants that latch on to a nearby crop plant and form a direct connection with the plant xylem, sapping vital energy from the plant to fuel its own flowering and seed-producing process. Once a field has been infested with seeds that lie dormant for up to 10 years, the parasites will dramatically reduce crop output for that field. According to some estimates, yields are reduced anywhere from 20-90%, with an average of 68% of crop losses. Crop losses are most severe in poor or underdeveloped regions, where the soil is typically of poor quality.

These parasitic plants affect agricultural fields throughout the world, although they are of particular concern on the African continent. Witchweeds (*Striga spp.;* and in particular the species *Striga hermonthica and Striga asiatica*) are the major plague of the Africa; some two-thirds of the cereal crop fields are infected with parasitic weed species. Affected crops include staples such as millet, maize, rice, sorghum, cowpea, and sugar cane. These parasites are not contained to Africa, however; in the Middle East, India, Europe and North America, affected crops typically include legumes, crucifers, tomato, sunflower, hemp, and tobacco. These plants are mainly targets of *Orobanche,* which is pervasive in North America, although *Striga asiatica* and *Striga gesnerioide* have been introduced as an invasive species in North Carolina, South Carolina,

and Florida, with spread that has been contained by strict quarantine of the area (Bouwmeester et al., 2003).

Because of the interest to crop production worldwide, life-cycle interplay and chemical signaling between host and parasite has been well-characterized. First, the roots of the host plant release a small molecule germination stimulant into the soil that activates the parasite seed, causing it to germinate and grow along a gradient towards the source of the stimulant. Successful attachment to a host plant is required within a few days or the plant die once it has exhausted its nutritional reserves. Once the plant attaches to the root, it forms a haustorium, a specialized attachment point that penetrates and connects the parasite permanently to either the host xylem (Striga) or phloem (Orobanche), sapping water and vital nutrients from the plant.

The identity of the germination stimulant was the subject of intense study in the 1990s. Since the initial discovery of +/- strigol (so named because of its identity as a germination stimulant for Striga), several different types of compounds had been shown to act as germination stimulants for different species. The major molecules shown to be germination stimulants are a family of strigolactones including +/- strigol, sorgolactone, alectrol, orobanchol and dihydrosorgeoleone. The synthetic strigolactone commonly used in research, GR24, is also a germination stimulant for Striga. The degree of selection between compounds and activity may explain the observation that different crop plants act differently on different parasitic species (Bouwmeester et al., 2003). Interestingly, these compounds are particularly efficacious at stimulating the

parasitic germination, inducing 50% seed germination at picomolar concentrations.

With such large losses attributed to parasitic plants, researchers and other organizations have been actively pursuing methods to reduce or eliminate Striga and Orobanche infestations, particularly on the African continent. Conventional herbicide application at the top layer of soil is not effective, as these drugs act on actively growing plants, and much of the damage is done before Striga emerges from the ground. Selective breeding for crop resistance to Striga has had some success, producing a resistant sorghum cultivar, although these plants are only partially resistant and not widely available. Fertilization of the soil, particularly phosphate fertilization, has attenuated Striga infection in many areas. A specific type of intercropping, known as "push-pull intercropping" has been utilized to pre-germinate the Striga seeds with the legume *Desmodium uncinatum* as intercrop, and is the most promising strategy to date and the strategy used to control Striga infestation in North and South Carolina along with extensive quarantine. Lastly, the German company BASF has launched its STRIGAWAY™ system that includes a maize variety mutagenized to be resistant to the patent herbicide Imazapyr. The company coats the seeds of the resistant maize with herbicide, resulting in a plant that grows with a circle of weed-free soil surrounding the base of the plant, effectively reducing Striga infection and improving crop output. However, these seeds are expensive, and intellectual property issues mean that farmers must sign contracts with BASF to

ensure that they will not save seeds, a limitation that makes the method ultimately not sustainable.

In addition to intercropping or breeding of generally resistant lines of crops, the ideal approach to reducing Striga infectivity may include the availability of a cheap, stable germination stimulant for Striga that can be applied early in the growing cycle to pre-germinate the Striga when no host plants are yet present, causing the plant to exhaust its small resource of energy and die before the host plants are set into the ground. The germination stimulant strigolactones themselves are unsuitable for this purpose as they are easily destabilized in water.

Structures of several strigolactone analogues have now been solved by NMR; the hormones have been revealed as caroteinoid-derived multi-ringed molecules as displayed below (See Figure 1.3). Structure-function analysis has identified the critical region of the structure for the hormone signaling function is the C-D ring linkage. Notably, this ether bond is particularly sensitive to Michael addition of water to the enol linkage and the subsequent elimination of the D-ring, producing the unstable nature of the molecule in aqueous solution (See Figure 1.3). One of the goals of our structure-function study of MAX2 bound to strigolactone is the identification of bonds within the hormone binding pocket that may accommodate a different linkage between the C- and D- rings that still provides for hormone function. I anticipate that intelligent design of strigolactones can provide successful modification of this backbone to produce a strigolactone agonist molecule that is more stable in aqueous solution.

After the identification of strigolactones, researchers questioned the natural role of "germination stimulant" in crop plant growth and development. Because of their severe detriment to crop growth and reproductive capabilities, it was clear that the induction of parasitic growth was not the primary purpose of its biosynthesis by the plant.

In 2005, a group of small molecules were identified and isolated in lipophilic fractions of root exudates of *Lotus japonicus*, as host-derived signals that were sufficient to induce hyphal branching in arbuscular mycorrhizal (AM) fungi (Akiyama et al., 2005). Hyphal branching increases contact surface between the host plant and the AM fungi, permitting greater uptake of phosphate and nitrogen resources for the plant. The "branching factor" was quickly identified as the parasitic plant germination factor strigolactone, providing the first evidence of a role of strigolactones for normal plant growth and development. AM fungi form symbiotic relationships with the roots of more than 80% of land plants. Even those plants that are capable of forming relationships with root nodule bacteria, the legumes, will release strigolactones to stimulate AM fungi in low phosphate conditions. Although the signal has evolved to initiate the formation of mycorrhizae with AM fungi and the plant root as positive symbiotic relationships, this signal has also been exploited by obligate parasites.

The identification of strigolactone regulation of AM fungal colonization tied together many different observations made regarding parasitic plant infection. Phosphate starvation increases the exudation of several compounds,

including strigolactones; the same condition also induced a greater proportion of the seeds of Orobanche to germinate. This could explain the suppressive effect of phosphate fertilization on parasitic weed germination. In fact, colonizing the soil with AM fungi has been shown to have a suppressive effect on infection of sorghum and maize by Striga.

The release of strigolactones is a major mechanism by which the plant effects change in its local environment to stimulate more effective uptake of phosphate and nitrogen by symbiotic fungi. This finding has implications for the types of Striga management methods that may be counterproductive. For example, breeding of low "germination stimulant" cultivars may be an insufficient solution: although these plants do not release strigolactones to induce Striga germination, their inability to signal to symbiotic fungi means that these plants will remain nutritionally limited, particularly in soil that is phosphate-depleted. In addition, association with symbiotic fungi provides additional benefits for the plant, including increased resistance to environmental stress.

Strigolactones have been detected released in the media surrounding the roots, or in the exudates, of many different plant species, including maize (*Zea mays*), sorghum (*Sorghum bicolor*), cotton (*Gossypium hirsutum*), and tomato (*Solanum lycopersicon*). These exudates can contain several different strigolactone metabolites, and different strigolactones may be released even when comparing between varietals of the same species. The symbiosis initiated by strigolactone production occurs throughout the plant kingdom and plays an essential role in plant biology. Because of the structure of the strigolactone

backbone, predictions of nearly 100 different strigolactone molecules that support the broadness of host specificity between AM fungi and host plant that has evolved over several hundred million years.

A ground-breaking paper, published in 2005, significantly changed the course of strigolactone research. Although strigolactones were classified previously as sesquiterpene lactones, further elucidation of the pathway for strigolactone synthesis revealed that strigolactones are derived from carotenoids, and are specifically caroteinoid-derived terpenoid lactones.

Far from the field of parasitic plants and AM fungi, researchers had been working on classifying an orthologous set of organismal mutants, *RAMOSUS* (rms) of pea (*Pisum sativum*), *MORE AXILLARY GROWTH* (MAX) of *Arabidopsis thaliana*, and *HIGH-TILLERING DWARF* (htd) of rice (*Oryza sativa*) (Domagalska and Leyser, 2011). These mutants show enhanced shoot branching, particularly the formation of axillary buds in the axil of the leaves which leads to subsequent outgrowth of the buds. Examination of this pathway, and careful evaluation of cytokinin, auxin, and abscisic acid in *rms* mutants, lead researchers to the conclusion that the phenotype was controlled by a novel hormone that was synthesized from the caroteinoid pathway. Many of the mutants encode CCDs (caroteinoid cleavage dioxygenases); for example, the *Arabidopsis* MAX3 locus encodes CCD7, MAX4 encodes CCD8. With the discovery that a hormone in the caroteinoid pathway controlled this group of mutants, and that strigolactones themselves were caroteinoids, the two areas of research dovetailed and were quickly united.

To unequivocally establish that these branching mutants were in fact defective in the strigolactone pathway, the mutants were genetically characterized for strigolactone sensitivity. Application of strigolactones to WT plants was found to inhibit tillering in rice; CDD7 and CDD8 d mutants of rice are deficient in production of strigolactones by LC-MS, are complemented by GR24, and are infected by fewer Striga seeds. Similarly, root exudates of rms1 mutants had significantly less ability to stimulate hyphal branching of AM fungi and stimulate less germination of Orobanche.

Of the different mutants, those that can be rescued by root grafting or by exogenous application of strigolactones were designated mutants in the hormone biosynthesis pathway. All mutants in hormone biosynthesis display reduced strigolactone production by the plant. By contrast, those mutants that cannot be rescued and who still produce normal or above-normal amounts of the hormone are not biosynthetic mutants, but mutants that have lost function in the later hormone-sensing step. These hormone-sensing mutants include MAX2, RMS4, and D3, all of which are orthologous F-box proteins that are similar to auxin receptor TIR1. MAX2 is the last enzyme identified in the "sensing" portion of the strigolactone pathway, and is therefore the most likely candidate for the strigolactone receptor. This is supported by the many other plant hormone pathways that utilize F-box protein ubiquitin ligases as hormone receptors, as well as the fact that no gene has been identified to act downstream of any of these proteins. This evidence together indicates that targeting of ubiquitin ligase

proteins by hormones appears to be favored across plant biology, and is likely to be conserved in the strigolactone pathway.

Strigolactones are unique among plant hormones in that they have such specific action, primarily regulating hyphal and shoot branching. This is in stark contrast to auxins, which are more pleiotropic and have a wide set of different activities and phenotypes that occur when the auxin system is depressed. It may be that strigolactones are simply more specialized as signalling molecules. However, MAX2 mutants have additional phenotypes that go beyond just increased branching, such as altered light responsiveness and senescence. Because of the common redundancy of enzymes in important metabolism pathways, it is possible that enzyme compensation causes these mutant plants to be leaky (where strigolactone synthesis is not abolished by any one mutant), or that MAX2 is used for signal transduction of another pathway.

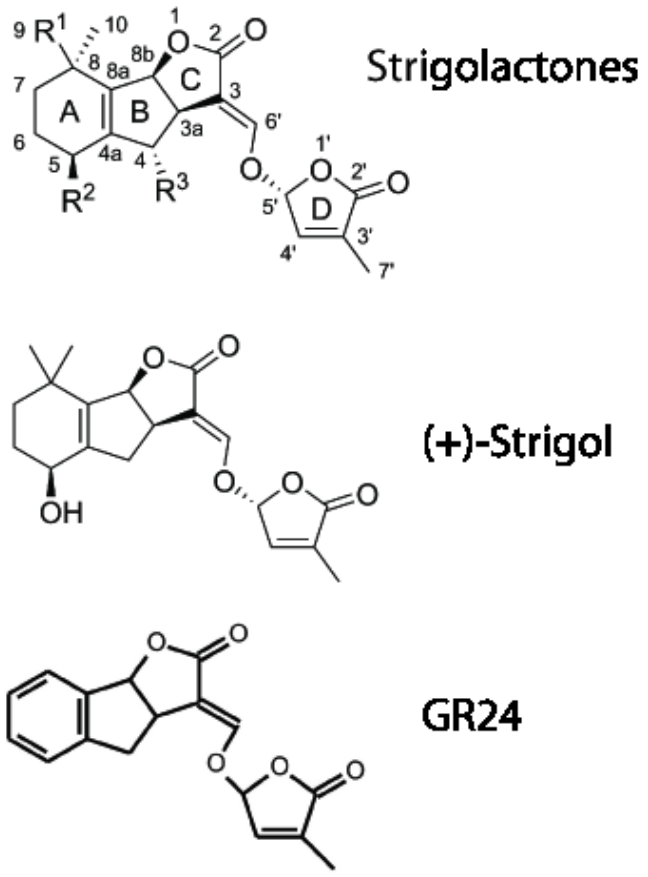

Figure 1.3 Strigolactone structural backbone. Strigolactone analogs are predicted to retain highest function in the C-D rings and linkage, which contains an unstable enol bond.

1.4 Jasmonate and COI1

The phytohormone jasmonate (JA) and its metabolites regulate a wide spectrum of plant physiology, participating in normal development and growth processes, as well as defense responses to environmental and pathogenic stressors (Browse, 2009). JA is activated upon specific conjugation to the amino acid L-isoleucine (Ile), which produces the highly bioactive hormonal signal, JA-Ile (Staswick and Tiryaki, 2004) that is functionally and structurally mimicked by the *Pseudomonas syringae* phytotoxin coronatine (Feys et al., 1994; Fonseca et al., 2009; Staswick and Tiryaki, 2004). The discovery of coronatine-insensitive mutants enabled the identification of CORONATINE INSENSITIVE 1 (COI1) as a key player in the JA pathway, with further implications of regulated proteolysis in JA perception and signal transduction (Xie et al., 1998).

COI1 is an F-box protein that functions as the substrate-recruiting module of the Skp1-Cul1-F-box protein (SCF) ubiquitin E3 ligase complex. Recent studies have identified the JASMONATE ZIM-domain (JAZ) family of transcriptional repressors as the SCF^{COI1} substrate targets, which associate with COI1 in a hormone-dependent manner (Chini et al., 2007; Thines et al., 2007; Yan et al., 2007). In the absence of hormone signal, JAZ proteins actively repress the transcription factor MYC2. In response to cues that up-regulate JA-Ile synthesis, the hormone stimulates the specific binding of JAZ proteins to COI1, leading to poly-ubiquitination and subsequent degradation of JAZ by the

26S proteasome. JAZ degradation relieves repression of MYC2 and likely other transcription factors, permitting the expression of JA-responsive genes (Chini et al., 2007; Lorenzo et al., 2004) The role of COI1-mediated JAZ degradation in JA signaling is analogous to auxin signaling through the receptor F-box protein TIR1, which promotes hormone-dependent turnover of the AUX/IAA transcriptional repressors (Dharmasiri et al., 2005; Kepinski and Leyser, 2005). Supported by its sequence homology and functional similarity to TIR1, COI1 has been assigned a critical role in the direct perception of the JA signal (Katsir et al., 2008; Yan et al., 2009).

Despite the importance of JA signaling in plant physiology, the molecular mechanism of JA perception remains elusive. Together with Dr. Xu Tan and Dr. Haibin Mao, I here present crystal structures of COI1 bound to JA-Ile or coronatine, as well as peptides of a bi-partite JAZ1 degron. Our structural and pharmacological studies reveal that the true JA receptor is in fact a co-receptor complex, consisting of the F-box protein COI1, the JAZ degron, and a newly discovered third component, inositol pentakisphosphate.

CHAPTER 2

COI1-JAZ complex as a jasmonate co-receptor

2.1 Results

To better characterize the pharmacology of JA perception, we used recombinant proteins and ^{3}H-coronatine to quantitatively define the functional components of the receptor system with an *in vitro* radioligand binding assay. From saturation binding experiments, we detected high affinity specific binding of ^{3}H-coronatine to COI1 in the presence of two different full-length JAZ proteins, JAZ6 and JAZ1 at a K_d of 68 nM and 48 nM, respectively (Fig. 2.1a,b). The highly active (3*R*,7*S*) isomer of JA-Ile (Fig. 2.1c), and the less active (3*R*,7*R*) isomer, compete with ^{3}H-coronatine for binding to the COI1-JAZ6 complex with K_i values of 1.8 μM and 18 μM, respectively (Fig. 2.2a). In contrast, ^{3}H-coronatine displayed no affinity to the JAZ proteins and exhibited only marginal binding to the F-box protein alone. Hormone binding to COI1 alone elicited < 2% binding signal relative to that of COI1-JAZ at a concentration that saturates the complex (300 nM) (Fig. 2.1a, Fig. 2.2b). This result, together with the observation that endogenous JA-Ile activates COI1-dependent gene expression in the nM range(Browse, 2009; Koo et al., 2009; Suza and Staswick, 2008), indicates that the COI1-JAZ complex, rather than COI1 alone, functions as the genuine high affinity JA receptor in a co-receptor form.

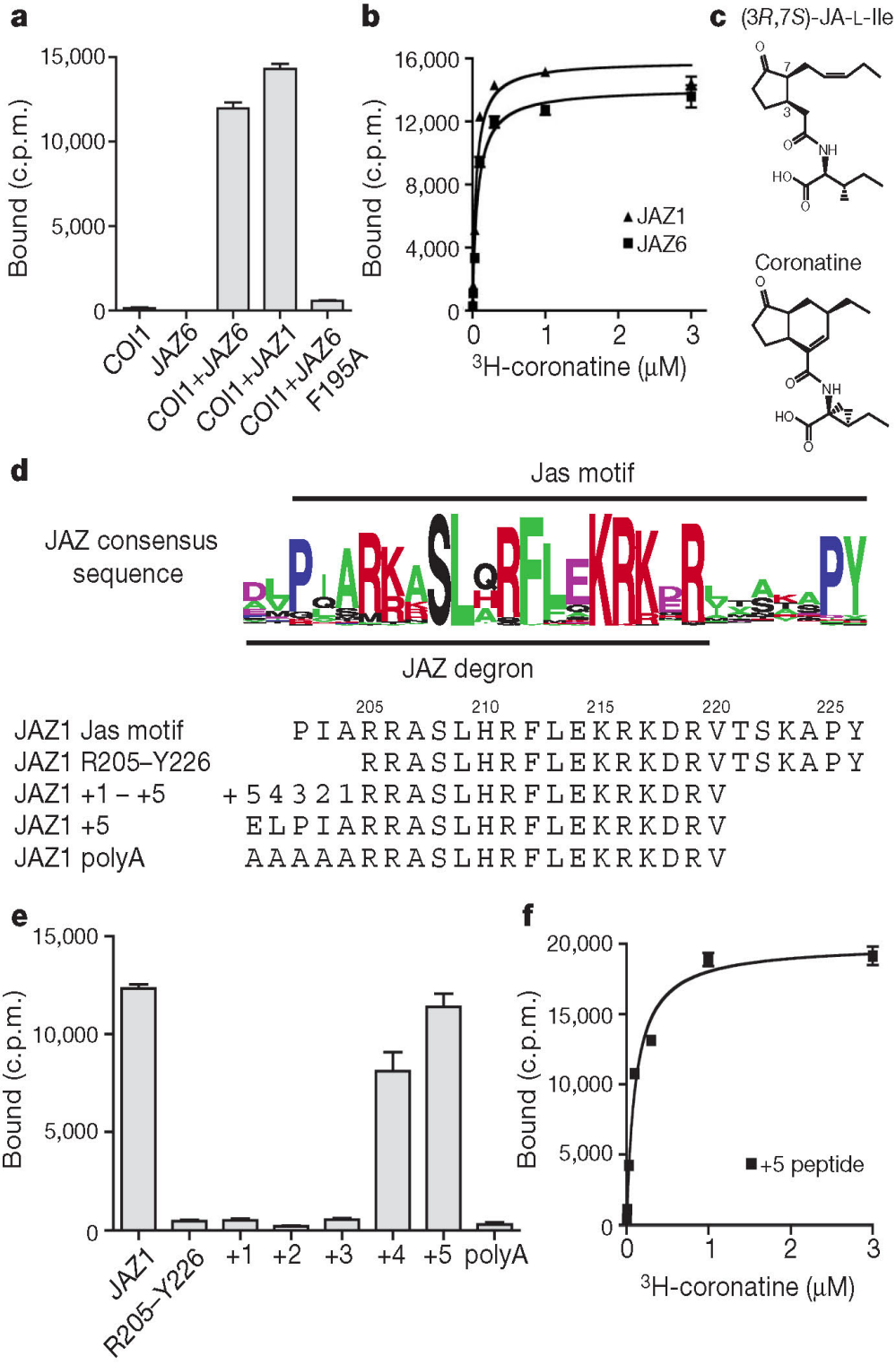
a
Bound (c.p.m.)
15,000
10,000
5,000
0
COI1
JAZ6
COI1+JAZ6
COI1+JAZ1
COI1+JAZ6 F195A
b
Bound (c.p.m.)
16,000
12,000
8,000
4,000
0
JAZ1
JAZ6
0 1 2 3
3H-coronatine (μM)
c
(3R,7S)-JA-L-Ile
Coronatine
d
Jas motif
JAZ consensus sequence
JAZ degron
205 210 215 220 225
JAZ1 Jas motif P I A R R A S L H R F L E K R K D R V T S K A P Y
JAZ1 R205–Y226 R R A S L H R F L E K R K D R V T S K A P Y
JAZ1 +1 – +5 + 5 4 3 2 1 R R A S L H R F L E K R K D R V
JAZ1 +5 E L P I A R R A S L H R F L E K R K D R V
JAZ1 polyA A A A A A R R A S L H R F L E K R K D R V
e
Bound (c.p.m.)
15,000
10,000
5,000
0
JAZ1
R205–Y226
+1 +2 +3 +4 +5 polyA
f
Bound (c.p.m.)
20,000
15,000
10,000
5,000
0
+5 peptide
0 1 2 3
3H-coronatine (μM)

Figure 2.1. COI1-ASK1 and JAZ proteins form a high-affinity JA co-receptor. a. Binding of tritium-labeled coronatine (300 nM) to recombinant COI1-ASK1 and JAZ proteins. b. Saturation binding of ^{3}H-coronatine to the complex of COI1-ASK1 in the presence of JAZ6 or JAZ1, with a K_d of 68±15 nM and 48±13 nM, respectively. c. Chemical structures of (3*R*,7*S*)-JA-Ile and coronatine. d. The consensus sequence of the Jas motif from 61 JAZ proteins from two monocot and three dicot plant species. Corresponding peptide sequences from JAZ1 in (e) are listed below. e. ^{3}H-coronatine binding at 300 nM to COI1 in the presence of a series of synthetic JAZ1 peptides with the N-terminus of R205-Y226 systematically extended as described in (d). f. Saturation binding of COI1-ASK1 and the JAZ1 +5 degron peptide, with a K_d of 108±29 nM. All results are the mean ± S.E. of two to three experiments performed in duplicate.

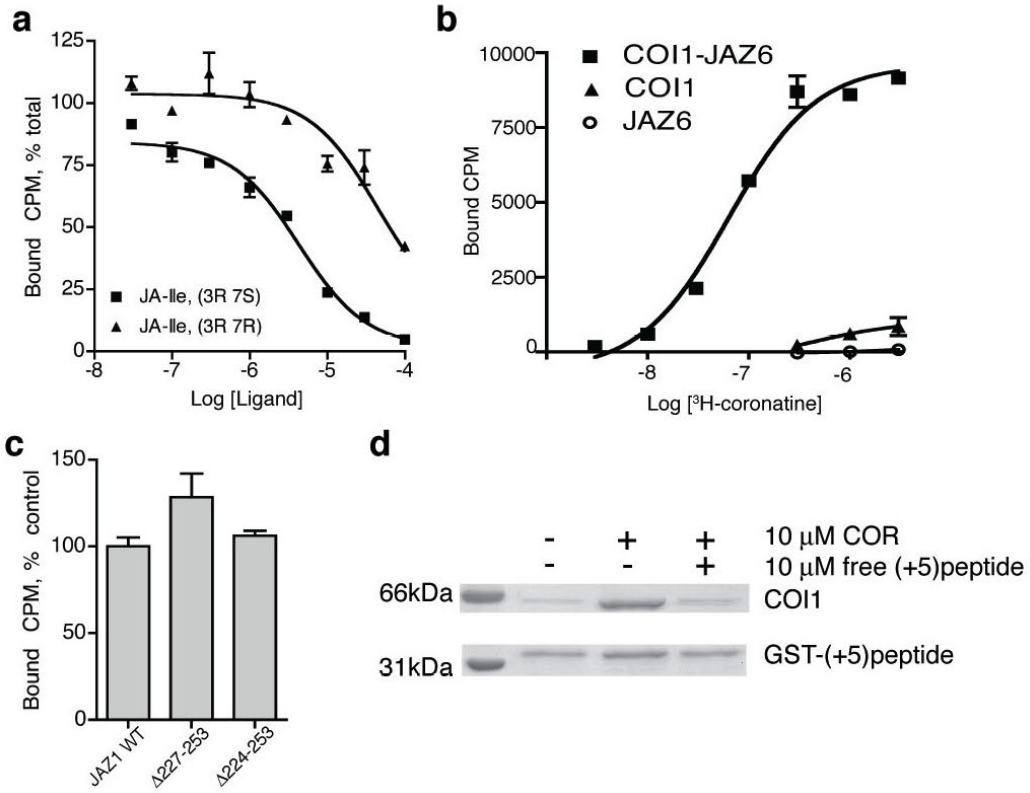

Figure 2.2. Radioligand binding and pull-down analysis of COI1-JAZ interaction. a. Competition binding of 100nM ^{3}H-COR with (3*R*, 7*S*)-JA-Ile, and (3*R*,7*R*)-JA-Ile at a Ki of 1.8± 0.6 μM and 18±19 μM, respectively. b. Saturation ^{3}H-coronatine binding curves (up to 3 μM ^{3}H-coronatine) of the COI1-JAZ6 complex, isolated COI1, and isolated JAZ6. Binding of ^{3}H-coronatine to the COI1-JAZ6 complex reached the level of saturation at 300 nM. At the same concentration of ^{3}H-coronatine, COI1 alone yielded <2% specific binding. c. Binding assays performed with 300 nM ^{3}H-coronatine and JAZ1 proteins truncated immediately after (Δ227-253) or before (Δ224-253) the PY motif. d. GST fused with the JAZ1+5 peptide (Glu200-Val220) can pull-down COI1 in a hormone-dependent manner. 10 μM free JAZ1+5 peptide can compete with this interaction.

We have previously mapped the COI1-binding region of the JAZ proteins to the C-terminal Jas motif, which is characterized by the $SLX_2FX_2KRX_2RX_5PY$ consensus sequence preceded by two consecutive basic residues (Chung and Howe, 2009; Melotto et al., 2008) (Fig. 2.1d). A single Ala mutation of the central strictly conserved phenylalanine residue in the Jas motif is sufficient to abolish the formation of the high affinity JA co-receptor (Fig. 2.1a). Previous studies showed that the highly conserved PY sequence at the C-terminus of the Jas motif plays a role in JAZ localization and stability *in vivo,* but is not required for ligand-dependent COI1-JAZ interaction (Chung et al., 2010; Chung and Howe, 2009; Grunewald et al., 2009). Consistent with these findings, truncation of the PY motif in JAZ1 has little effect on the *in vitro* ligand binding activity (Fig. 2.2c).

To further map the minimal region of the Jas motif required for high affinity ligand binding with COI1, we replaced the recombinant protein with synthetic peptides of JAZ1 in the ligand binding assay (Fig. 2.1d, e). A 22-amino-acid JAZ1 peptide (Arg205–Tyr226) spanning the central conserved Jas motif plus the two N-terminal basic residues was not sufficient to form the high affinity JA co-receptor with COI1, suggesting that amino acids N-terminal to Arg205 also participate in the COI1-JA interaction. Because several JAZ proteins exhibit sequence homology in this region (Fig. 2.1d), we tested a series of JAZ1 peptides in which the N-terminus was systematically extended by one amino acid. Strikingly, inclusion of four but not three amino acids N-terminal

to Arg205 allows ligand-dependent co-receptor formation, whereas addition of the fifth residue (Glu200) to the JAZ1 peptide permits ^{3}H-coronatine binding with a K_d comparable to that of the full-length JAZ1 protein (Fig. 2.11e, f). Despite the sequence variation among different JAZ members in this region, only select amino acids are functional in this five amino acid extension, as a penta-alanine sequence fails to elicit the same effect (Fig. 2.1e). Together, these results indicate that the JAZ1 protein uses a minimal sequence (Glu200–Val220) within the Jas motif, which consists of a highly conserved central and C-terminal region and a more variable N-terminal region, to interact with COI1 and perceive the JA signal. Consistent with our *in vitro* ligand binding data, the minimal sequence in JAZ1 is sufficient for coronatine-induced COI1-JAZ1 interaction (Fig. 3.1d). Therefore, we conclude that the interactions among COI1, coronatine, and the JAZ1 peptide are highly cooperative and that the short Glu200–Val220 sequence functions as the JAZ1 degron.

2.2. Materials and Methods

2.2a. Protein preparation.

The full-length *Arabidopsis thaliana* COI1 and ASK1 were co-expressed as a glutathione S-transferase (GST)-fusion protein and an untagged protein, respectively, in Hi5 suspension insect cells. The COI1-ASK1 complex was isolated from the soluble cell lysate by glutathione affinity chromatography. After on-column tag cleavage by tobacco etch virus protease, the complex was further purified by anion exchange and gel filtration chromatography and

concentrated by ultrafiltration to 12–18 mg mL^{-1}. Full-length JAZ substrate proteins were expressed as 6xHIS-fusion proteins in *Escherichia coli* and purified on Ni-NTA resin with subsequent dialysis into 20 mM Tris-HCl, pH=8.0, 200 mM NaCl, and 10% glycerol. For truncation mutants, a stop codon was introduced in JAZ1 proteins using the Quick-Change II site-directed mutagenesis kit (Stratagene). Synthetic JAZ degron peptides were prepared by United Biochemical Research, Inc. JAZ degron fusion peptides were prepared with N-terminal 6x-HIS tag and C-terminal glutathione S-transferase (GST)-fusion tag and expressed in *Escherichia coli*. The protein was isolated by glutathione affinity resin for pull-down assay with untagged COI1-ASK1 complex.

2.2b Hormone and IP reagents.

^{3}H-coronatine was synthesized by Amersham (Katsir et al., 2008). Coronatine was purchased from Sigma; JA-Ile conjugates were chemically synthesized as previously described (Ogawa and Kobayashi, 2011). Synthetic inositol phosphates were purchased as sodium salts from Cayman Chemicals. $InsP_6$ was purchased from Sigma.

2.2c Radioligand binding assay.

Radioligand binding was assayed on purified proteins, with 2 mg COI1-ASK1 complex and JAZ proteins at 1:3 molar ratio, and/or 10 mM synthetic peptides. Reactions were prepared in 100 mL final volume and in a binding

buffer containing 20 mM Tris-HCl, 200 mM NaCl, and 10% glycerol. Saturation binding experiments were conducted with serial dilutions of ^{3}H-coronatine in binding buffer. Non-specific binding was determined in the presence of 300 mM coronatine. Competition binding experiments were conducted with serial dilutions of JA-Ile in the presence of 100 nM ^{3}H-coronatine with nonspecific binding determined in the presence of 300 mM coronatine. Total binding was determined in the presence of vehicle only. Two-point binding experiments were performed in the presence of 100 nM or 300 nM ^{3}H-coronatine with nonspecific binding determined in the presence of 300 mM coronatine. Following incubation with mixing at 4°C, all samples were collected with a cell harvester (Brandel, Gaithersburg, MD) on polyethyleneimine (Sigma)-treated filters. Samples were incubated in liquid scintillation fluid for >1 hour before counting with a Packard Tri-Carb 2200 CA liquid scintillation analyzer (Packard Instrument Co. Inc., Rockville, MD). Saturation binding experiments were analyzed by non-linear regression, competition binding experiments by non-linear regression with K_i calculation as per the method of Cheng and Prousoff (Cheng and Prusoff, 1973), and concentration-response data by sigmoidal dose-response curve fitting, all using GraphPad Prism version 4.00 for MacOSX.

CHAPTER 3

Jasmonate-binding pocket on COI1

3.1 Results

To elucidate the structural mechanism by which the COI1-JAZ1 co-receptor senses JA, we crystallized and determined the structures of the COI1-ASK1-JAZ1 degron peptide complex together with either (3*R*,7*S*)-JA-Ile or coronatine (Table 1). The crystal structure of COI1 reveals a TIR1-like overall architecture (Tan et al., 2007), with an N-terminal tri-helical F-box motif bound to ASK1 and a C-terminal horseshoe-shaped solenoid domain formed by 18 tandem leucine-rich repeats (LRRs; Fig. 3.1a, b). Similar to TIR1, the top surface of the COI1 LRR domain has three long intra-repeat loops (Loop-2, 12, and 14) that are involved in hormone and polypeptide substrate binding. Unlike TIR1, however, a fourth long loop (Loop-C) in the C-terminal capping sequence of the COI1 LRR domain folds over Loop-2, partially covering it from above (Fig 3.1b, c).

Despite their similar overall fold, COI1 has evolved a hormone-binding site that is distinct from TIR1. Configured in between Loop-2 and the inner wall of the LRR solenoid, the ligand-binding pocket of COI1 is exclusively encircled by amino acid side chains (Fig. 3.1d-f). Many of the pocket-forming residues on COI1 are large in size and carry a polar head group (Fig. 3.2). These properties allow them to mold a binding pocket into a specific shape while forming close interactions with each chemical moiety of the ligand. These close interactions

are critical to proper hormone-sensing of the complex — in yeast two-hybrid assays, mutation of any of these large side-chain amino acids on COI1 is sufficient to disrupt the interaction of COI1 with JAZ1 in the presence of coronatine (Fig. 3.3).

In the binding pocket, both JA-Ile and coronatine sit in an "upright" position with the keto group of their common cyclopentanone ring pointing up and forming a triangular hydrogen bond network with Arg496 and Try444 of COI1 at the pocket entrance (Fig. 3.1d-f). Without the JAZ degron peptide bound, the keto group of the ligand is accessible to solvent (Fig. 3.1g). The rest of the cyclopentanone ring of both JA-Ile and coronatine is sandwiched between the aromatic groups of Phe89 and Tyr444 of COI1, stabilized by hydrophobic packing. The cyclohexene ring of coronatine provides a rigid surface area for close packing with Phe89, whereas the more flexible and extended pentenyl side chain of JA-Ile is more loosely accommodated by a hydrophobic pocket formed by Ala86, Phe89, and Leu91 from Loop-2 as well as Leu469 and Trp519 from the LRRs (Fig. 3.4a). Differences at this interface likely explain the approximately 10-fold higher affinity of coronatine over (3*R*,7*S*)-JA-Ile, as detected in our binding assays.

Table 1. Crystallographic data collection and refinement statistics

	COI1-ASK1-JAZ1 R205-Y226-coronatine	COI1-ASK1-JAZ1 degron-coronatine	COI1-ASK1-JAZ1 degron-JA-Ile
Data collection			
Space group	P21	P21	P21
Cell dimensions			
a, *b*, *c* (Å)	121.8, 221.5, 148.5	123.2, 220.8, 149.5	122.3, 220.8, 148.7
α, β, γ (°)	90.0, 104.5, 90.0	90.0, 104.5, 90.0	90.0, 104.5, 90.0
Resolution (Å)	2.80 (2.80 – 2.90)	3.35 (3.35 – 3.41)	3.18 (3.18 – 3.31)
R_{sym}	0.103 (0.816)	0.119 (0.700)	0.088 (0.462)
$I/\sigma I$	16.7 (2.0)	14.0 (2.1)	17.2 (2.8)
Completeness (%)	100 (100)	92.9 (94.6)	97.0 (93.3)
Redundancy	3.9 (3.8)	3.6 (3.3)	3.1 (2.7)
Refinement			
Resolution (Å)	50 – 2.80	50 – 3.35	50 – 3.18
No. reflections	174,966	95,997	116,337
R_{work}/R_{free}	0.235/0.270	0.225/0.270	0.223/0.264
R.m.s deviations			
Bond lengths (Å)	0.008	0.010	0.010
Bond angles (°)	1.676	1.271	1.556

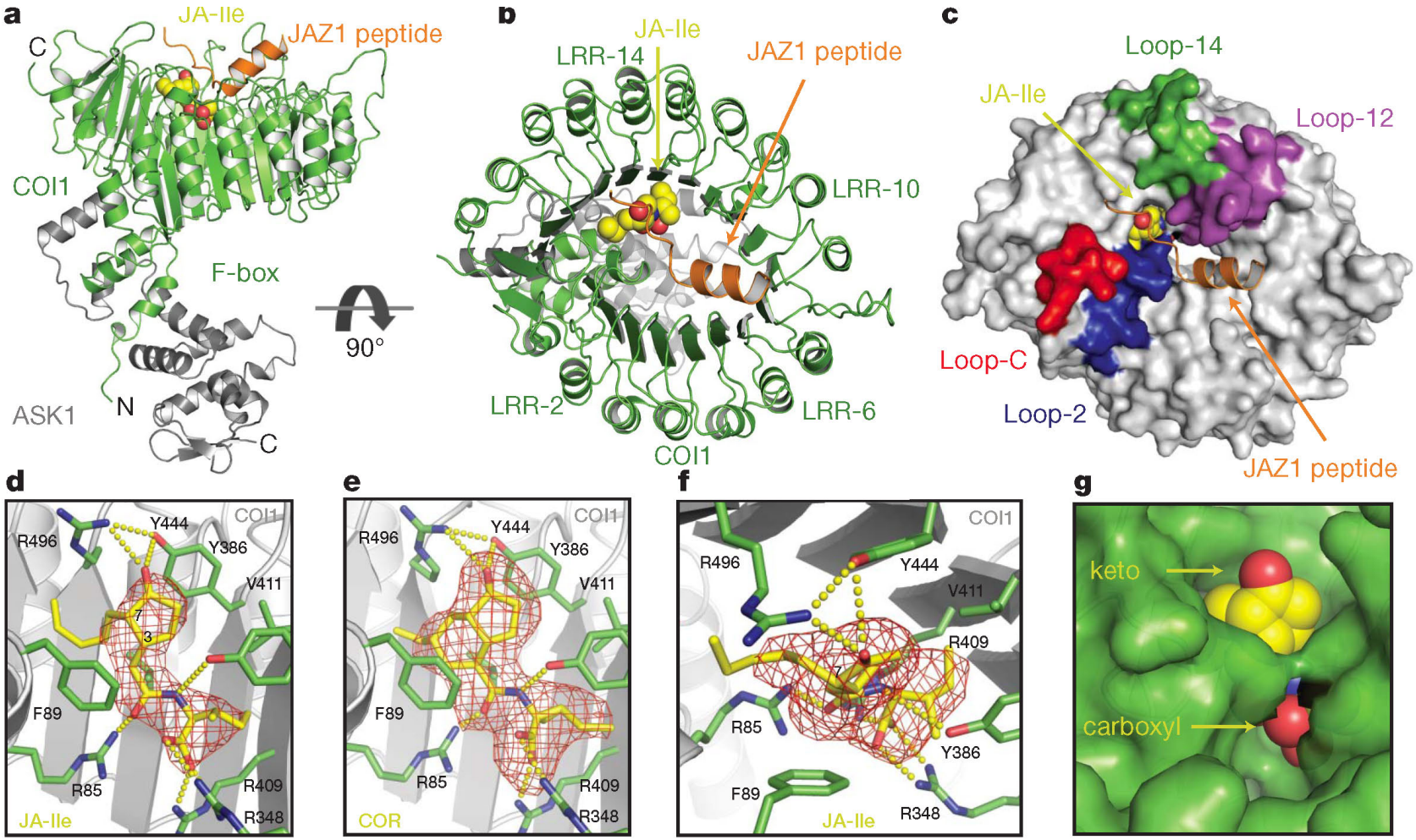
a
JA-Ile
JAZ1 peptide
C
COI1
F-box
ASK1
N
C
90°
b
JA-Ile
LRR-14
JAZ1 peptide
LRR-10
LRR-2
LRR-6
COI1
c
Loop-14
JA-Ile
Loop-12
Loop-C
Loop-2
JAZ1 peptide
d
COI1
Y444
R496
Y386
V411
F89
R85
R409
R348
JA-Ile
e
COI1
Y444
R496
Y386
V411
F89
R85
R409
R348
COR
f
COI1
R496
Y444
V411
R409
R85
Y386
F89
R348
JA-Ile
g
keto
carboxyl

Figure 3.1. Crystal structure of the COI1-ASK1 complex with JA-Ile and the JAZ degron peptide. a, b. COI1-ASK1 (green and grey ribbon, respectively), with JAZ degron peptide (orange ribbon) and (3*R*,7*S*)-JA-Ile in yellow spacefill. c. Surface representation of COI1 (grey) with Loops-2 (blue), -12 (purple) and -14 (green) forming the JA-Ile binding pocket. d, e. Side view of (3*R*,7*S*)-JA-Ile (JA-Ile) and coronatine (COR) binding. Hormones are shown as stick models, along with positive F_o-F_c electron density, calculated before they were built into the model (red mesh). Hydrogen bond and salt bridge networks are shown with yellow dashes. f. Top view of JA-Ile pocket showing the F_o-F_c electron density, calculated before JA-Ile was built into the model (red mesh). The electron density of the pentenyl side chain of (3*R*,7*S*)-JA-Ile cannot accommodate the (3*R*,7*R*)-JA-Ile side chain, which is constrained by the chiral configuration at the C7 position. g. When bound to COI1, JA-Ile (yellow spacefill) is solvent accessible at both the keto group (top) and carboxyl group (bottom).

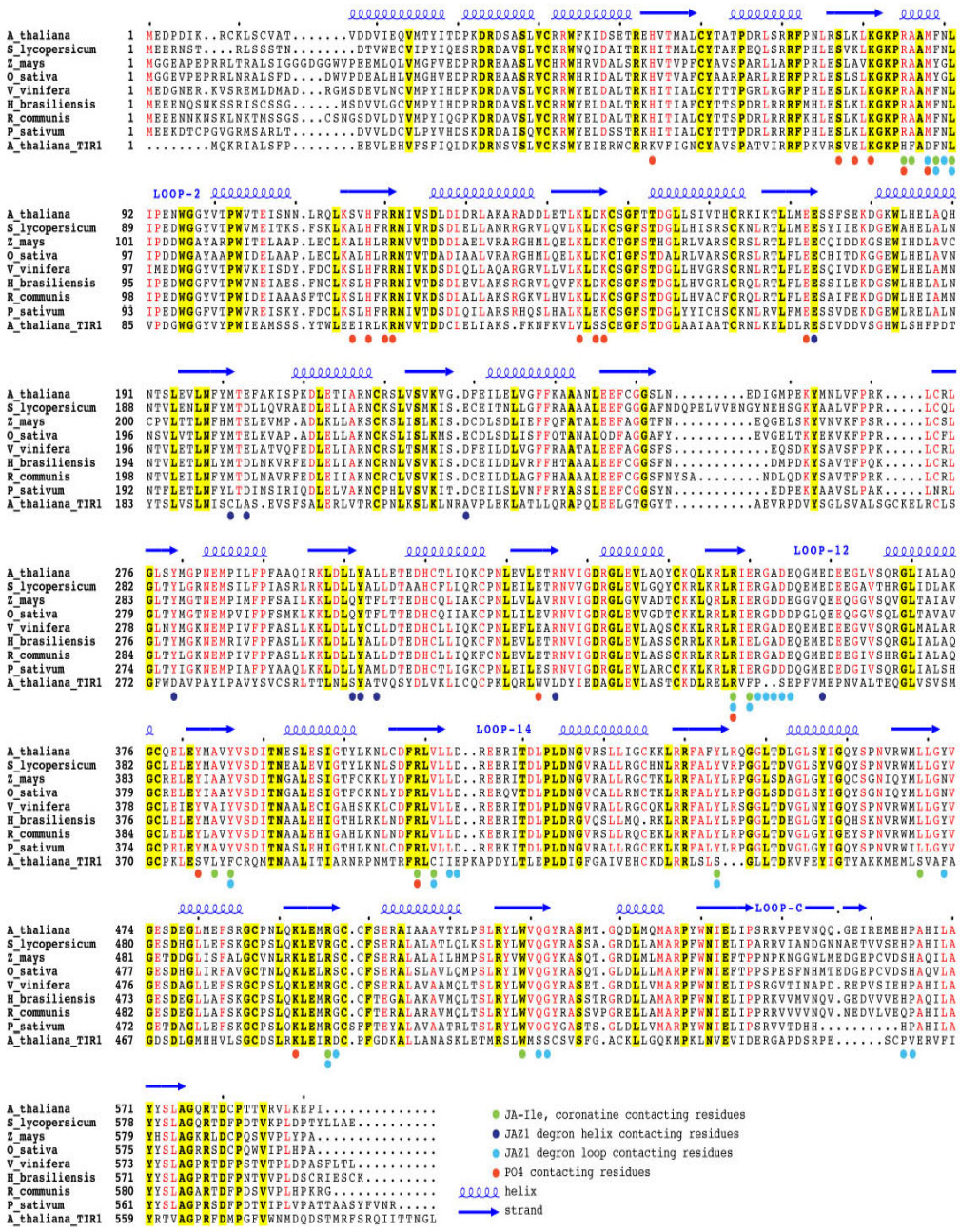
LOOP-2
LOOP-12
LOOP-14
LOOP-C
JA-Ile, coronatine contacting residues
JAZ1 degron helix contacting residues
JAZ1 degron loop contacting residues
PO4 contacting residues
helix
strand

Figure 3.2 Sequence alignment and structural annotation of COI1 orthologues. COI1 orthologues of select plant species are aligned, together with *Arabidopsis thaliana* TIR1. Secondary structure elements as determined in the crystal structure of COI1-ASK1-JAZ1 degron peptide-JA-Ile complex are shown on top of *Arabidopsis thaliana* COI1 sequence. Critical ligand-, phosphate-, and substrate-contacting residues are indicated by colored dots as described in the key.

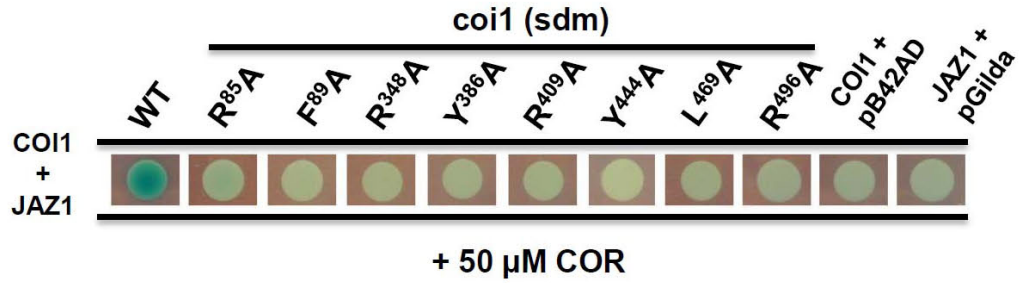

Figure 3.3 Residues within the JA-Ile binding pocket of COI1 are critical for ligand-induced COI1-JAZ1 interaction. Site-directed mutagenesis and yeast two-hybrid assay were performed as described in the method section. “sdm” indicates site-directed mutantions.

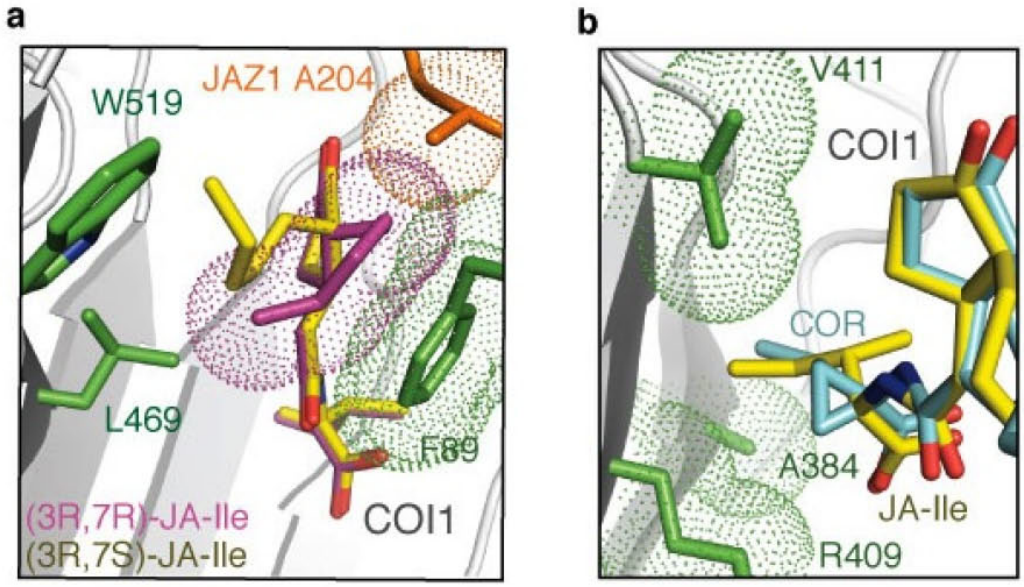

Figure 3.4 Hydrophobic binding pockets for JA-Ile on COI1. a. Side view of the COI1 pocket accommodating the pentenyl side chain of (*3R, 7S*)-JA-Ile (yellow stick). The pentenyl side chain of (*3R, 7S*)-JA-Ile (magenta stick) is modeled on the structure of (*3R, 7S*)-JA-Ile and rotated around C7-C8 bond to minimize collision with JAZ1 Ala204 and COI1 Phe89. The electron clouds of nearby COI1 (green) and JAZ1 (orange) side chains as well as the pentenyl side chain of (*3R, 7S*)-JA-Ile (magenta) are shown in dot form. Ala86 and Leu91 of COI1 blocking the front view of the pocket are omitted for clarity. b. Side view of (*3R- 7S*)-JA-Ile (yellow stick), and coronatine (cyan stick), showing a hydrophobic pocket that accommodates both the aliphatic isoleucine portion of JA-Ile and the cyclopropane ring of coronatine.

Deeper in the ligand binding pocket, the common amide and carboxyl groups of JA-Ile and coronatine bind to the bottom of the binding site by forming a salt bridge and hydrogen bond network with three basic residues of COI1, Arg85, Arg348, and Arg409 (Fig. 3.1d, e). Together, these arginine residues constitute the charged floor of the ligand pocket. Tyr386 reinforces the interactions from above by making a hydrogen bond with the amine group of the ligand. In doing so, Tyr386 approaches the cyclopentanone ring of the ligand, narrowing the pocket entrance, and creating a hydrophobic cave below. The rest of the basin is carved out by Val411, Ala384, and the aliphatic side chain of Arg409 (Fig. 3.4b). The ethyl-cyclopropane group of coronatine and the isoleucine side chain of JA-Ile can both comfortably fit in this space due to their similar size and hydrophobicity. The nature of the cave explains the preference of COI1 for JA conjugates containing a moderately-sized hydrophobic amino acid (Katsir et al., 2008). Although most of the ligand is buried inside the binding site, the keto group at the top and the carboxyl group at the bottom remain exposed, available for additional interactions with the JAZ portion of the co-receptor (Fig. 3.1g).

3.2 Materials and Methods

3.2a Crystallization, data collection, and structure determination.

The crystals of the COI1-ASK1-JAZ1 peptide complexes bound to either coronatine or JA-Ile were grown at 4°C by the hanging-drop vapor diffusion method with 1.5 ml protein complex samples containing COI1-ASK1, JAZ1

peptide, and hormone compound at 1:1:1 molar ratio mixed with an equal volume of reservoir solution containing 100 mM BTP, 1.7–1.9 M ammonium phosphate, 100 mM NaCl, pH=7.0. Diffraction quality crystals were obtained by the micro-seeding method at 4°C. The crystals all contain eight copies of the complex in the asymmetric unit. The data sets were collected at the BL8.2.1 beamline at the Advanced Light Source in Lawrence Berkeley National Laboratory as well as the GM/CA-CAT 23 ID-B beamline at the Advanced Photon Source in Argonne National Laboratory using crystals flash-frozen in the crystallization buffers supplemented with 15%–20% ethylene glycol at -170°C. Reflection data were indexed, integrated, and scaled with the HKL2000 package. All crystal structures were solved by molecular replacement using the program Phaser(Adams et al., 2002) and the TIR1-ASK1 structure as search model. The structural models were manually built in the program O (Jones et al., 1991) and refined using CNS (Brünger et al., 1998) and PHENIX (Adams et al., 2002). All final models have 96–98% of residues in the favoured region and 0% in disallowed region of the Ramachandran plot.

CHAPTER 4

Structural roles of the bipartite JAZ degron

4.1 Result

The JAZ1 degron peptide adopts a bipartite structure with a loop region followed by an α-helix to assemble with the COI1-JA complex. The hallmark of the JAZ1 degron is the N-terminal five amino acids identified in the radioligand binding assay. In a largely extended conformation, this short sequence lies on top of the hormone-binding pocket and simultaneously interacts with both COI1 and the ligand, effectively trapping the ligand in the pocket (Fig. 4.1a, b). At the N-terminal end, Leu201 of the JAZ1 peptide is embedded in a hydrophobic cavity presented by surface loops on top of COI1 (Fig. 4.1c). At the C-terminal end, Ala204 of JAZ1 uses its short side chain to pack against the keto group of the ligand and Phe89 of COI1 (Fig. 4.1c, Fig. 3.4a). The same alanine residue of JAZ1 also donates a hydrogen bond through its backbone amide group to the keto moiety of the ligand emerging from the pocket (Fig. 4.1c). The middle region of the five amino acid sequence is secured to the COI1-JA complex through a hydrogen bond formed between the backbone carbonyl of Pro202 in JAZ1 and the ligand-interacting COI1 residue Arg496, which is critical for hormone-dependent COI1-JAZ interaction (Fig. 3.3). In agreement with its important role in forming the JA-Ile co-receptor, this short N-terminal region of the JAZ1 degron completely covers the opening of the ligand-binding pocket, conferring high affinity binding to the hormone. The close interaction between

the hormone and the co-receptor complex provides a plausible structural explanation for the favorable binding of (3*R*,7*S*)-JA-Ile isomer, as the stereochemistry at the 7 position of (3*R*,7*R*)-JA-Ile may place the aliphatic chain unfavorably close to nearby JAZ1 and COI1 residues (Fig. 3.4a).

Within the JAZ1 degron, two conserved basic residues, Arg205 and Arg206, were previously shown to play an important role in hormone-induced COI1 binding (Melotto et al., 2008). In the structure, Arg205 contributes to COI1 binding by directly interacting with Loop-12, whereas Arg206 points in the opposite direction and inserts deeply into the central tunnel of the COI1 solenoid. Approaching the bottom of the ligand-binding pocket, the guanidinium group of the Arg206 side chain joins the three basic COI1 residues that form the pocket floor and interacts directly with the carboxyl group of the ligand (Fig. 4.1d). Thus, the N-terminal seven amino acids (ELPIARR) of the JAZ1 degron peptide acts as a clamp that wraps the ligand-binding pocket from top to bottom, closing it completely (Fig. 4.1b).

The highly conserved C-terminal half of the JAZ1 degron forms an amphiphathic α-helix that strengthens JAZ1-COI1 interaction by binding to the top surface of the COI1 LRR domain, adjacent to the ligand-binding site (Fig. 4.1a). With its N-terminal end directly packing against Loop-2 of COI1, the Jas motif helix blocks the central tunnel of the COI1 LRR solenoid like a plug. The N-terminal half of the Jas motif helix is characterized by three hydrophobic residues, Leu209, Phe212, and Leu213, which are aligned on the same side of the helix and form a hydrophobic interface with COI1 (Fig. 4.1e). By soaking

the COI1-ASK1 crystals with coronatine and a sufficiently high concentration of JAZ1 degron peptide lacking the N-terminal ELPIA sequence, we were able to trap a complex formed by COI1, coronatine, and the isolated Jas motif helix in the crystal (Table 1). This suggests that the α-helix may provide a low affinity anchor for docking the JAZ protein on COI1. In support of this idea, single amino acid mutations at the complementary surface on COI1 readily disrupt hormone-induced COI1-JAZ1 interaction (Fig. 4.1f).

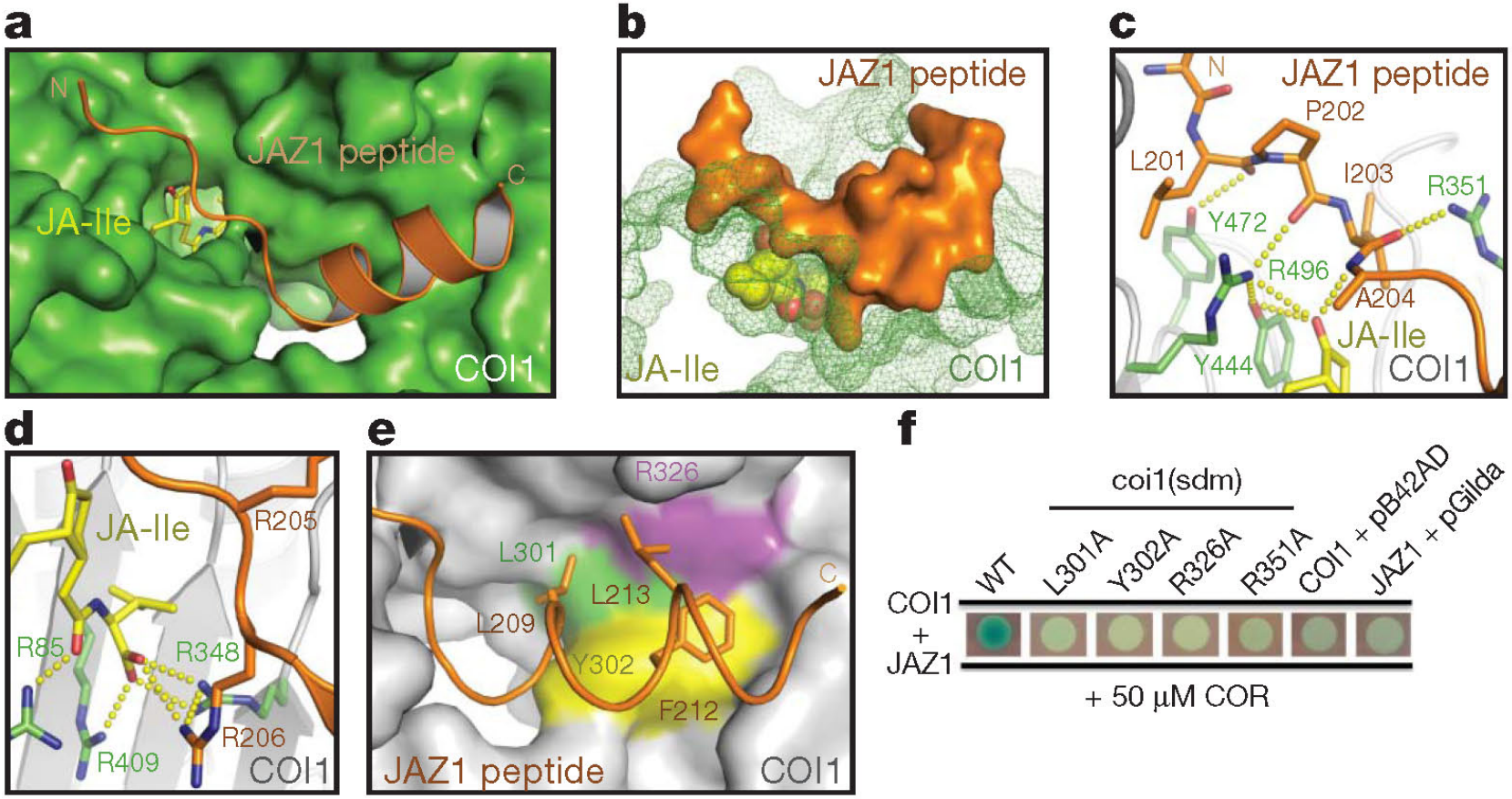
a
N
JAZ1 peptide
C
JA-Ile
COI1
b
JAZ1 peptide
JA-Ile
COI1
c
N
JAZ1 peptide
P202
L201
I203
R351
Y472
R496
A204
JA-Ile
Y444
COI1
d
JA-Ile
R205
R85
R348
R206
R409
COI1
e
R326
L301
L213
C
L209
Y302
F212
JAZ1 peptide
COI1
f
coi1(sdm)
WT
L301A
Y302A
R326A
R351A
COI1 + pB42AD
JAZ1 + pGilda
COI1
+
JAZ1
+ 50 µM COR

Figure 4.1 The bi-partite JAZ degron peptide. a. Top view of the complete JAZ1 degron peptide (orange) bound to COI1 (green) and JA-Ile (yellow). b. Side view and surface representation of the JAZ peptide, which acts as a clamp to lock JA-Ile in the pocket. c. Interactions of the N-terminal region of the JAZ1 degron with COI1 and JA-Ile. Hydrogen bonds are shown with yellow dashes. d. Structural role of the Arg206 residue from the JAZ1 degron in coordinating the carboxyl group of JA-Ile with three basic residues of the COI1 ligand pocket floor. e. Top view of the amphiphathic JAZ1 degron helix bound to COI1 with three hydrophobic residues of JAZ1 shown in orange stick, and COI1 residues in colored surface representation. f. Coronatine-induced interactions of wild type and mutant COI1 with JAZ1 detected by yeast two-hybrid assay (sdm: site-directed mutants). Blue color indicates interaction.

CHAPTER 5

Inositol pentakisphosphates as a cofactor of COI1

5.1 Result

The crystal structure of TIR1 revealed an unexpected inositol hexakisphosphate ($InsP_6$) molecule bound in the center of the protein underneath the auxin-binding pocket (Tan et al., 2007). The sequence homology between COI1 and TIR1 suggests that COI1 might also contain a similar small molecule. Prior to crystallization, we analyzed the recombinant COI1-ASK1 complex by structural mass spectrometry (MS). Nano-electrospray mass spectra of the intact COI1-ASK1 complex revealed two populations differing by a mass of ~568 Da, indicating that a small molecule was indeed co-purified with the proteins (Fig. 4a, Fig. 5.2). The MS-derived molecular weight of the unknown compound is different from the mass of $InsP_6$ (651 Da) but matches that of an inositol pentakisphosphate ($InsP_5$) molecule. Unfortunately, MS analyses of either the native COI1-ASK1 complex or the denatured proteins were unable to achieve direct mass analysis of the small molecule.

To investigate the identity of the unknown compound, we first estimated that the molecule contains four or five phosphate groups by ^{31}P nuclear magnetic resonance (NMR) of trypsin-digested COI1-ASK1 complex (data not shown). To unequivocally identify the unknown molecule, we set out to purify it away from the COI1-ASK1 complex in a quantity sufficient for ^{1}H NMR analysis.

The high phosphate content of the molecule allowed us to trace it through a multi-step purification procedure (Fig. 5.1b). Following isolation of 150 nanomoles of the purified small molecule, we acquired a series of 1D and 2D NMR data, including a highly informative homonuclear total correlation (TOCSY) spectrum. The observed chemical shifts and TOCSY cross-peak patterns are clearly characteristic of inositol phosphates (Fig. 5.1c). A comparison with previously reported NMR spectra of various inositol phosphates established that the unknown compound is either D- or L-inositol (1,2,4,5,6) pentakisphosphate, or Ins(1,2,4,5,6)P_5 (Fig. 5.1c) (Stephens et al., 1991). This conclusion was further supported by the TOCSY spectrum of synthetic Ins(1,2,4,5,6)P_5 (Fig. 5.1d) and subsequently acquired negative-ion electrospray ionization-MS spectrum of the compound (Fig. 5.3).

Consistent with the binding of a small molecule cofactor, the crystal structure of COI1 showed strong unexplained electron densities clustered in the middle of the COI1 LRR domain. Like $InsP_6$ in TIR1, these extra densities in COI1 are located directly adjacent to the bottom of the ligand-binding pocket of the JA co-receptor, interacting with multiple positively charged COI1 residues (Fig. 5.1e). Unexpectedly, these islands of electron density cannot be explained by an Ins(1,2,4,5,6)P_5 molecule. Instead, their intensity, overall symmetry, and poor connectivity strongly suggest that they belong to multiple free phosphate molecules. Because a high concentration of ammonium phosphate was used as the major precipitant for crystallizing the JA co-receptor, we postulate that the $InsP_5$ molecule co-purified with COI1 was later displaced by phosphate

molecules in the crystallization drops. In support of this scenario, the concave surface of the COI1 solenoid fold surrounding the phosphates is highly basic and decorated with residues conserved in plant COI1 orthologues, indicating a functionally important surface area (Fig. 5.1f, Fig. 3.2, 5.4).

5.2 Materials and Methods

5.2a Inositol phosphate purification.

Phenol was melted at 68°C and equilibrated with equal parts 0.5 M Tris-HCl, pH=8.0 until a pH of 7.8 was reached. The equilibrated phenol was then topped with 0.1 volume 100 mM Tris-HCl, pH=8.0 and stored at 4°C. For extraction, 30–40 mg of 1 mg mL^{-1} COI1-ASK1 protein was mixed in small batches with equal parts equilibrated phenol at room temperature. The samples were inverted and incubated for 30 minutes until phase separation occurred. With 30 seconds vortexing, the samples were incubated at room temperature for 30 minutes and spun at 15,000 RPM for 5 minutes. The aqueous phase was removed as a primary extraction. Equal parts of a solution containing 25 mM Tris-HCl, pH=8.0 was added to the phenol and collected as above as a secondary extraction. The primary and secondary extractions were then combined and diluted 10x in 25 mM Tris-HCl, pH=8.0, then further purified by gravity flow on Q sepharose high performance anion exchange resin (GE Healthcare). Following column wash with 10x column volumes 0.1N formic acid, stepwise elution was performed with 2x column volumes of 0.1N formic acid (Thermo Scientific) with increasing concentrations of ammonium formate (Sigma), from 0 to 2M.

Fractions were analyzed for phosphate content by wet-ashing method with perchloric acid in Pyrex culture tubes (13x 100mm). Typically samples of 50–100 µl were ashed with 100–200 µl 70% perchloric acid (purified by redistillation, Sigma). Ashing was performed by heating the sample over a Bunsen-type burner with continuous shaking to prevent bumping. When the sample stopped emitting white smoke, the reaction was considered complete and then heated to dryness. 500 µl of distilled water was added to the room temperature tubes and vortexed. 100 µl samples containing up to 10 nmole inorganic phosphate were assayed for phosphate by a modification of a published procedure (Sadrzadeh et al., 1993). 125 µl of acid molybdate color reagent was added and the samples were incubated, covered, at room temperature for 12–14 hr (overnight) for full color development (total volume 225µl). Plates were read at 650 nm and unknowns were determined from the linear regression of the standard curve (0–10 nmole NaH_2PO_4 per well). All assays were done in triplicate. Final fractions containing phosphate were combined and lyophilized repeatedly to remove residual ammonium formate.

5.2b Structural mass spectrometry analysis of the intact protein complex.

Nano-electrospray ionization mass spectrometry (MS) and tandem MS (MS/MS) experiments were performed on a Synapt HDMS instrument. Prior to MS analysis, 50 µl of a 16 mg mL^{-1} solution of COI1-ASK1 in 20 mM Tris-HCl pH=8, 0.2 M NaCl and 5 mM DTT, was buffer-exchanged twice into 0.5 M ammonium acetate solution by using Bio-Rad Biospin columns. To improve

desolvation during ionization, samples were diluted 1:4 in 0.5 M ammonium acetate and isopropanol was added to a final concentration of 5%. Typically an aliquot of 2 µl solution was loaded for sampling via nano-ESI capillaries which were prepared in house from borosilicate glass tubes as described previously (Nettleton et al., 1998). The conditions within the mass spectrometer were adjusted to preserve non-covalent interactions. The following experimental parameters were used: capillary voltage up to 1.26 kV, sampling cone voltage 150 V and extraction cone voltage 6 V, MCP 1590. For tandem MS experiments peaks centered at m/z 4,564 and 4,588 were selected in the quadrupole and collision energy up to 65 V was employed. Argon was used as a collision gas at maximum pressure. All spectra were calibrated externally by using a solution of cesium iodide (100 mg mL^{-1}). Spectra are shown with minimal smoothing and without background subtraction.

5.2c Nuclear magnetic resonance (NMR) analysis

NMR spectra were acquired on a Varian INOVA600 spectrometer equipped with a cold probe using 200 mM samples of purified compound X or synthetic inositol (1,2,4,5,6) pentakisphosphate (Cayman Chemical) dissolved in D_2O. TOCSY spectra were acquired with mixing times of 35 or 50 ms, processed with NMRPipe (Delaglio et al., 1995) and visualized with NMRView (Johnson, 2004).

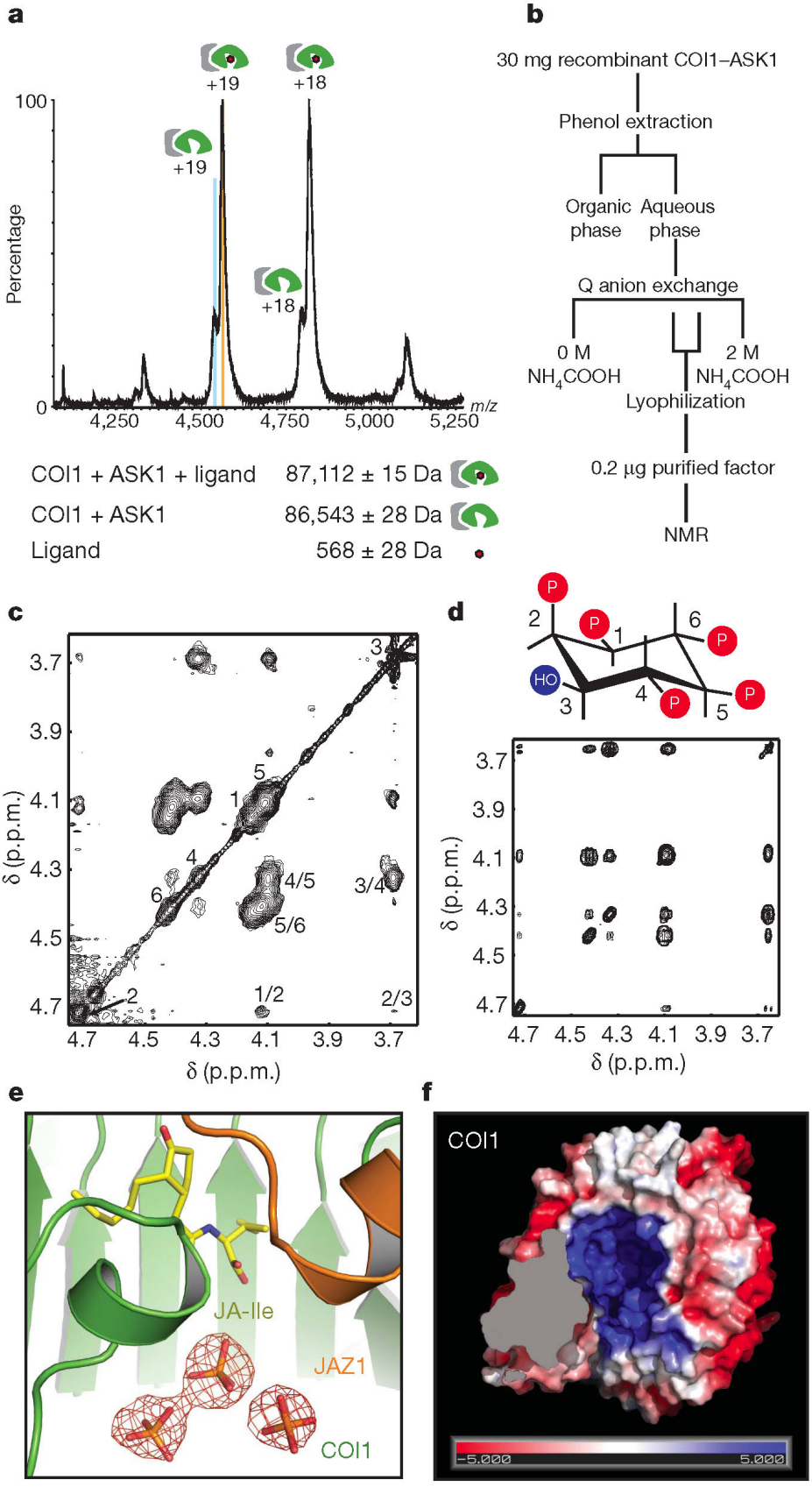
a
100
0
Percentage
+19
+18
+19
+18
4,250
4,500
4,750
5,000
5,250
m/z
COI1 + ASK1 + ligand 87,112 ± 15 Da
COI1 + ASK1 86,543 ± 28 Da
Ligand 568 ± 28 Da
b
30 mg recombinant COI1–ASK1
Phenol extraction
Organic phase
Aqueous phase
Q anion exchange
0 M NH4COOH
2 M NH4COOH
Lyophilization
0.2 µg purified factor
NMR
c
δ (p.p.m.)
3.7
3.9
4.1
4.3
4.5
4.7
1
2
3
4
5
6
1/2
2/3
3/4
4/5
5/6
d
P
HO
1
2
3
4
5
6
e
JA-Ile
JAZ1
COI1
f
COI1
−5.000
5.000

Figure 5.1 Identification of an inositol pentakisphosphate cofactor in COI1. a. Nano-electrospray MS of the intact COI1-ASK1 complex. Low intensity charge series corresponds in mass to the cofactor-free COI1-ASK1 complex. High intensity charge series corresponds to cofactor-bound COI1-ASK1 complex. b. Optimized cofactor purification scheme. c. Proton TOCSY spectrum of the purified cofactor. Numbers along the diagonal indicate the positions of the six protons of Ins(1,2,4,5,6)P_5. The cross-peaks corresponding to direct couplings are labeled. Other cross-peaks correspond to relayed connectivities. d. TOCSY spectrum of a synthetic Ins(1,2,4,5,6)P_5 as a standard. e. Islands of positive F_o-F_c electron density (red mesh) below the hormone-binding pockets, which likely belong to inorganic phosphate molecules from the crystallization solutions that displace $InsP_5$ from the $InsP_5$-binding site. f. Bottom view of a surface electrostatic potential representation of COI1 from positive (blue) to negative (red).

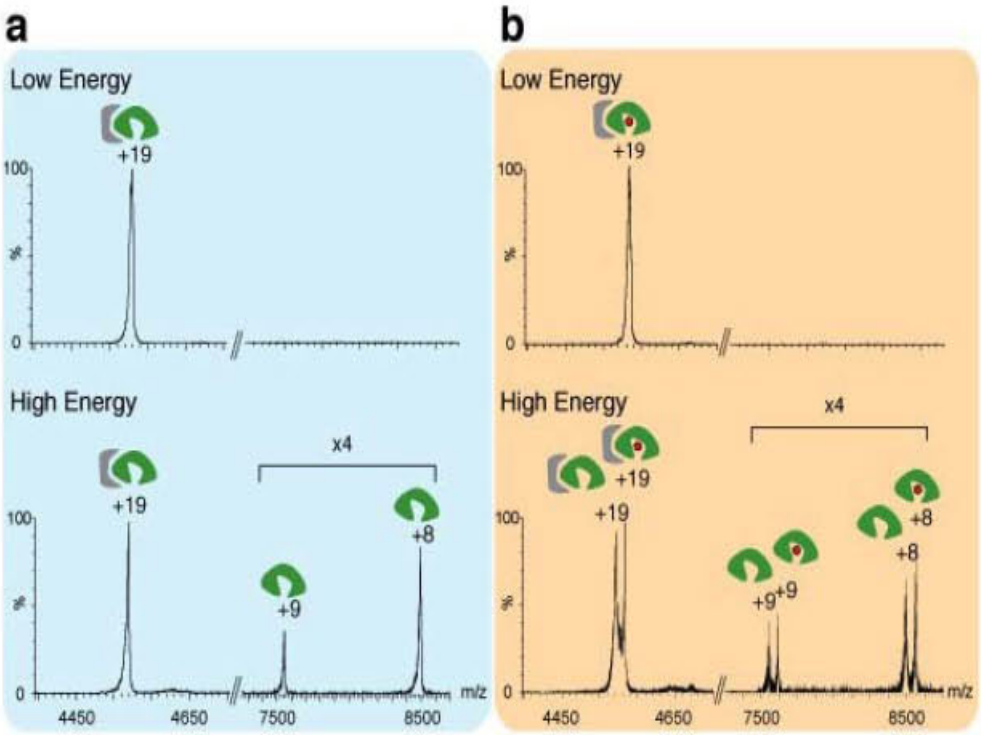

COI1 + ASK1 + Ligand	87,112 ± 15 Da	
COI1 + ASK1	86,543 ± 28 Da	
COI1 + Ligand	68,518 ± 4 Da	
COI1	67,952 ± 5 Da	
ASK1	18,511 ± 0.03 Da	
Ligand	568 ± 28 Da	

Figure 5.2 Structural mass spectrometry analysis of the COI1-ASK1 complex. a. Isolation at 4564 m/z of the 19+ charge state for tandem MS analysis, (shown in blue shown in Fig. 4a in main text). Both at low and high collision energy, only one population of the complex is apparent, corresponding to COI1-ASK1. At high collision energy, the complex dissociates into its different subunits and one population of COI1 appears in the spectrum, with a calculated mass of 67,944 ± 1 Da, which is in agreement with the theoretical mass of COI1, 67,947 Da. **b**. MS/MS spectrum showing the dissociation products of ions isolated at 4588 m/z, (shown in orange in Fig. 4a in main text). At low collision energy, only one form of the complex is apparent, corresponding to COI1-ASK1-ligand. However, elevating the collision energy releases some of the bound ligand and results in the appearance of a stripped COI1-ASK1 complex. The theoretical mass of the apo COI1-ASK1 complex is 86,458 Da, and is in close agreement with the observed mass of 86,543 ± 28 Da. The mass of the COI1-ASK1-ligand complex was found to be 87,112 ± 15 Da, suggesting that the mass of the ligand is around 568 ± 28 Da. The fact that both masses carry a charge of +19 indicates a neutral loss of the ligand, therefore it can not be detected in the spectrum. At high collision energy, some of the complex dissociates into its different subunits and two populations of COI1 appear in the spectrum. The smaller form, with a calculated mass of 67,952 ± 5 Da, fits the theoretical mass of COI1, 67,946.5 Da, whereas the other population, with a calculated mass of 68,518 ± 4 Da, corresponding to COI1-ligand, suggest that the mass of the ligand is around 568 ± 5 Da.

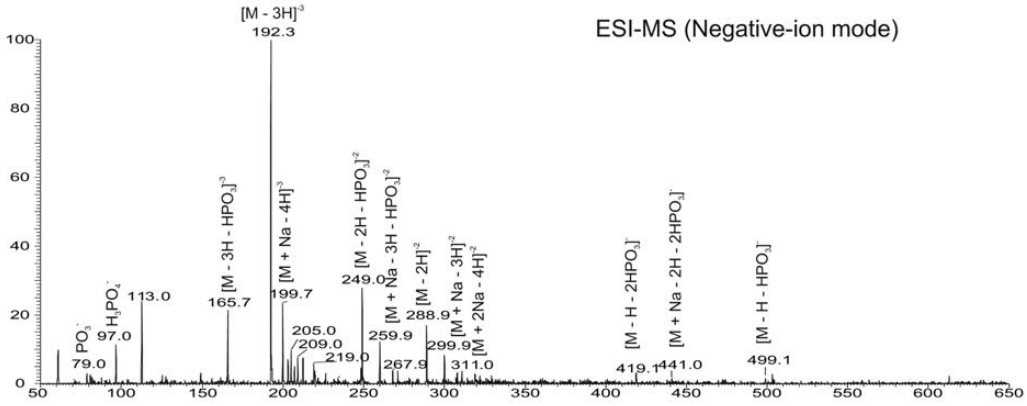

Ions observed for IP5 by negative-ion ESI-MS

m/z	structure
499	$[M - H - HPO_3]^-$
441	$[M + Na - 2H - 2HPO_3]^-$
419	$[M - H - 2HPO_3]^-$
311	$[M + 2Na - 4H]^{-2}$
300	$[M + Na - 3H]^{-2}$
289	$[M - 2H]^{-2}$
271	$[M + 2Na - 2H - 2HPO_3]^{-2}$
268	$[M + K - 3H - 2HPO_3]^{-2}$
259.9	$[M + Na - 3H - HPO_3]^{-2}$
249	$[M - 2H - HPO_3]^{-2}$
219	$[M + Na - 3H - 2HPO_3]^{-2}$
212	$[M + Na + K - 5H]^{-3}$
209	$[M - 2H - 2HPO_3]^{-2}$
207	$[M + 2Na - 5H]^{-3}$
203	$[M + Na - 4H]^{-3}$
199.7	$[M + Na - 4H]^{-3}$
192.3	$[M - 3H]^{-3}$
165.7	$[M - 3H - HPO_3]^{-3}$
97	$H_2PO_4^-$
79	PO_3^-

Figure 5.3 Mass spectrometry analysis of Ins(1,2,4,5,6)P_5 purified from recombinant COI1-ASK1. The negative-ion ESI-MS spectrum of the unknown is shown, which contained the major ion at m/z 192.3 ((579.8951 – 3x1.0078)/3), corresponding to the $[M - 3H]^{3-}$ ion of inositol pentakisphosphate ($InsP_5$), and the ion at m/z 288.9 ((579.8951 – 2x1.0078)/2), corresponding to the $[M - 2H]^{2-}$ ion of $InsP_5$, and the $[M - H]^-$ ion expected at m/z 579.9 was absent. The ions seen at m/z 199.7 and 207.1 correspond to the sodiated ions of $InsP_5$ seen as the $[M + Na - 4H]^{3-}$, and $[M + 2Na - 5H]^{3-}$ ions, respectively; and the ions at m/z 299.9 and 311.9 correspond to the $[M + Na – 3H]^{2-}$ and $[M + 2Na – 4H]^{2-}$ ions, respectively. The spectrum also contains ions at m/z 499 ($[M – H – HPO_3]^-$), 419 ($[M – H – 2HPO_3]^-$), and 441 ($[M + Na – 2H – 2HPO_3]^-$), arising from various losses of the phosphate residues of the molecule. The presence of the ion at m/z 499 (579.9 – HPO_3) is consistent with the observation of the ions at m/z 249 ($[M - 2H - HPO_3]^{-2}$), 259.9 ($[M + Na -3H - HPO_3]^{-2}$), and 165.7 ($[M - 3H - HPO_3]^{-3}$), representing the various deprotonated $InsP_4$ seen as doubly and triply charged anions. The ion at m/z 419 represents a deprotonated $InsP_3$ arising from loss of two HPO_3 residues; while the ion at m/z 441 represents a monosodiated $InsP_3$ anion. The presence of the ions at m/z 419 and 441 are also consistent with the observation of the doubly charged ions at m/z 209 and 219, corresponding to the $[M - 2H - 2HPO_3]^{-2}$ and $[M + Na - 3H - 2HPO_3]^{-2}$ ions, respectively. The assignments of the ions observed are listed the table. These ions were also observed for Ins(1,2,3,4,5)P_5 and Ins(1,2,4,5,6)P_5 standards, when subjected to ESI under the same condition, indicating that the unknown compound is an

$InsP_5$. This $InsP_5$ structure is further confirmed by the MS^n (n = 2,3,4,5) mass spectra of the $[M - 3H]^{3-}$ ion at m/z 192.3 and of the $[M - 2H]^{2-}$ ion at m/z 288.9 deriving from the unknown compound and from the Ins(1,2,3,4,5)P_5 and Ins(1,2,4,5,6)P_5 standards.

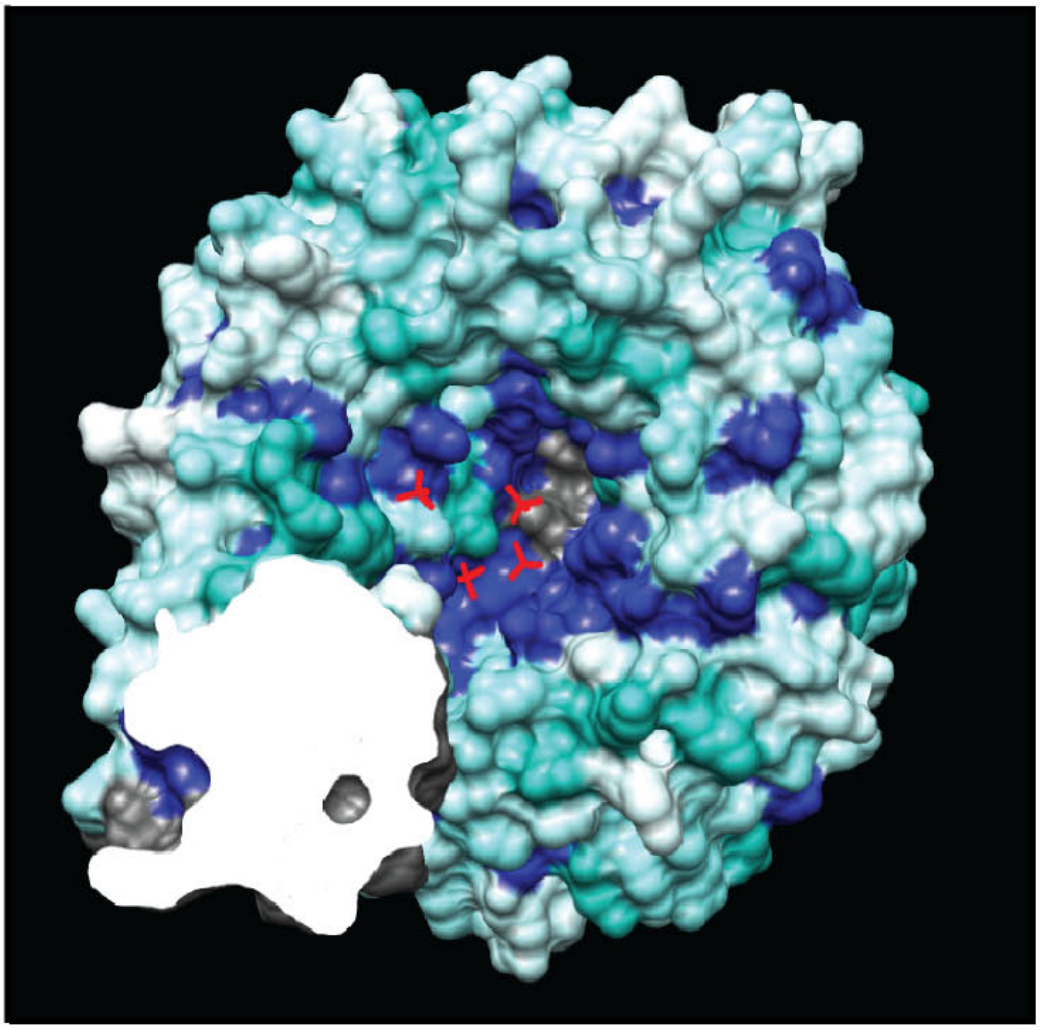

Figure 5.4. Surface conservation mapping of COI1. Conservation mapping of COI1 surface based on sequences of COI1 orthologues from 9 different species (*A. thaliana, H. brasiliensis, R. communis, P. trichocarpa, V. cinifera, P. sativum, S. lycopersicum, Z. mays,* and *O. sativa.*). Dark blue, light blue, and white surface regions indicate 98-100%, 60-98%, and <60% conservation, respectively. The F-box portion of COI1 and its associated ASK1 are curved out for clarity reasons. Four phosphate molecules bound to COI1 are shown by red sticks. JAZ1 peptide and ASK1 are shown in grey.

CHAPTER 6

InsP5 potentiates jasmonate perception by COI1-JAZ1

6.1 Result

The highly selective co-purification of two different inositol phosphates, $InsP_5$ and $InsP_6$, with two homologous plant hormone receptors, COI1 and TIR1, implies that the proper function of the two F-box proteins might require the binding of specific inositol phosphates. To assess the functional role of Ins(1,2,4,5,6)P_5 in the COI1-JAZ1 co-receptor, we took advantage of our crystallographic observation and developed a protocol to strip the co-purified $InsP_5$ from COI1 without denaturing the protein. The resulting COI1-ASK1 complex was then tested in a ligand binding-based reconstitution assay. As shown in Fig. 6.1a, untreated COI1 formed a high affinity JA co-receptor with JAZ1. Addition of exogenous Ins(1,2,4,5,6)P_5 did not significantly change its activity. In contrast, the dialyzed COI1 sample completely lacked ligand binding by itself and showed only trace activity in the presence of JAZ1. Supplementation with either synthetic Ins(1,2,4,5,6)P_5 (Fig. 6.1b) or the purified and NMR-analyzed $InsP_5$ sample (data not shown) rescued the interaction in a dose-dependent manner and with an EC_{50} of 27 nM (Fig. 6.1c). From this reconstitution result, we conclude that Ins(1,2,4,5,6)P_5 binding is crucial for the JA co-receptor to perceive the hormone with high sensitivity.

Although further effort is needed to reveal how $InsP_5$ binds to COI1, a close examination of the phosphate molecules in the available COI1 structure

suggests a mechanism by which the inositol phosphate molecule may modulate the activity of the JA co-receptor. Among four COI1-bound phosphates, one stands out by binding at a critical position in the JA co-receptor. This phosphate molecule interacts simultaneously with four basic residues at the bottom of the ligand-binding pocket, namely Arg206 in the JAZ1 degron and the three COI1 arginine residues that form the floor of the pocket. As a result, a tetragonal bipyramidal interaction network is formed among four molecules at the core of the JA co-receptor assembly. The four arginines from COI1 and JAZ1 sit at the four corners of the central plane, interacting with the hormone above and the phosphate below (Fig. 6.1f). As the free phosphate molecule likely mimics the action of a phosphate group on $InsP_5$, this four-molecule junction, together with additional phosphate-COI1 interactions seen in the crystal, conceivably represents the structural basis for $InsP_5$ potentiation of the JA co-receptor. Consistent with this interpretation, coronatine-induced formation of a COI1-JAZ1 complex was readily abolished by mutations of select COI1 residues adjacent to the phosphates, but not in contact with the hormone (Fig. 6.2).

We used the reconstitution assay to further investigate the specificity of JA co-receptor regulation by inositol phosphates (Fig. 6.1d). Intriguingly, inositol (1,4,5,6) tetrakisphosphate supports the activity of the COI1-JAZ1 co-receptor, whereas the second messenger signaling molecule inositol (1,4,5) triphosphate does not. Addition of a phosphate to $InsP_5$, which gives rise to $InsP_6$, is also not favorable for activity. Although saturation binding of ^{3}H-coronatine is stimulated by both $Ins(1,2,4,5,6)P_5$ and $InsP_6$ with similar K_d

values (30 nM and 37 nM, respectively), the two inositol phosphates yield drastically different B_{max} values for coronatine binding, indicating that $InsP_6$ is significantly less efficacious in activating the co-receptor despite having equal affinity as Ins(1,2,4,5,6)P_5 (Fig. 6.1e). Functional selectivity of COI1 for the inositol phosphate cofactor is consistent with the conservation of the putative inositol phosphate-binding site, which is distinct in amino-acid sequence from the $InsP_6$-binding site in TIR1 (Tan et al., 2007)(Fig. 3.2).

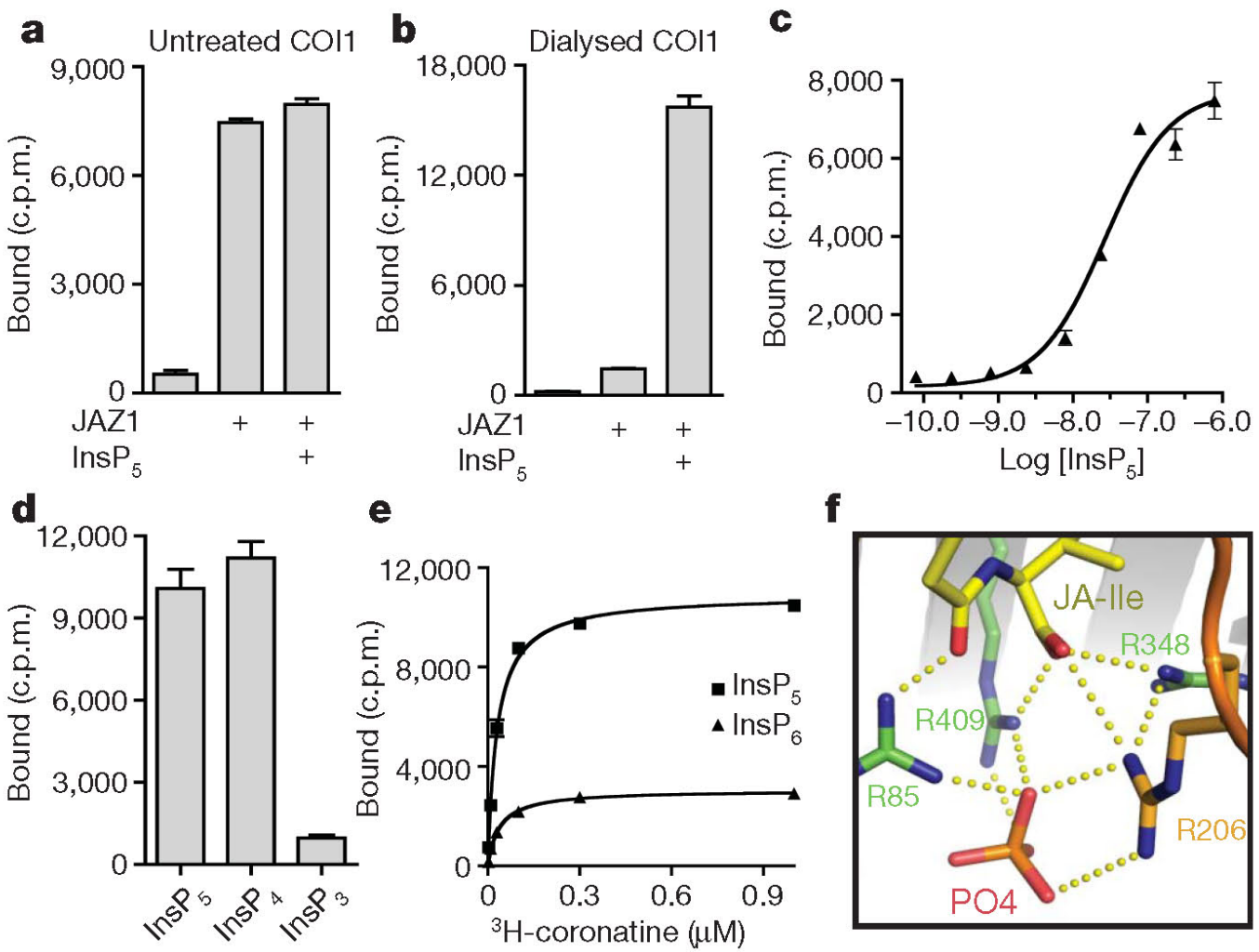
a
Untreated COI1
Bound (c.p.m.)
9,000
6,000
3,000
0
JAZ1 + +
InsP5 +
b
Dialysed COI1
Bound (c.p.m.)
18,000
12,000
6,000
0
JAZ1 + +
InsP5 +
c
Bound (c.p.m.)
8,000
6,000
4,000
2,000
0
–10.0 –9.0 –8.0 –7.0 –6.0
Log [InsP5]
d
Bound (c.p.m.)
12,000
9,000
6,000
3,000
0
InsP5 InsP4 InsP3
e
Bound (c.p.m.)
12,000
8,000
4,000
0
InsP5
InsP6
0 0.3 0.6 0.9
3H-coronatine (μM)
f
JA-Ile
R348
R409
R85
R206
PO4

Figure 6.1 Inositol phosphate is an essential component of the COI1-JAZ co-receptor. a. Binding of ^{3}H-coronatine at 100 nM to a complex of COI1 and JAZ1, with addition of 1 μM synthetic Ins(1,2,4,5,6)P_5 ($InsP_5$). b. With extensive dialysis to remove the co-purified $InsP_5$ cofactor, 100 nM ^{3}H-coronatine no longer binds dialyzed COI1 in the presence of JAZ1. Synthetic Ins(1,2,4,5,6)P_5 rescues binding. c. Ins(1,2,4,5,6)P_5 rescues the binding of 100 nM ^{3}H-coronatine to dialyzed COI1-ASK1 in the presence of JAZ1 with an EC_{50} of 27±12 nM. d. Binding assays performed with 100 nM ^{3}H-coronatine, dialyzed COI1, and 1 μM synthetic Ins(1,2,4,5,6)P_5 ($InsP_5$), Ins(1,4,5,6)P_4 ($InsP_4$), or Ins(1,4,5)P_3 ($InsP_3$). e. Saturation binding of ^{3}H-coronatine to dialyzed COI1 in the presence of 1 μM of Ins(1,2,4,5,6)P_5 ($InsP_5$) and Ins(1,2,3,4,5,6)P_6 ($InsP_6$) at a K_d of 30±5 nM and 37±8 nM, respectively. All results are the mean ± S.E. of up to three experiments performed in duplicate. f. A phosphate-binding site in the complex structure reveals an interwoven hydrogen bond network that may explain the mechanism by which the InsP cofactor potentiates the JA co-receptor.

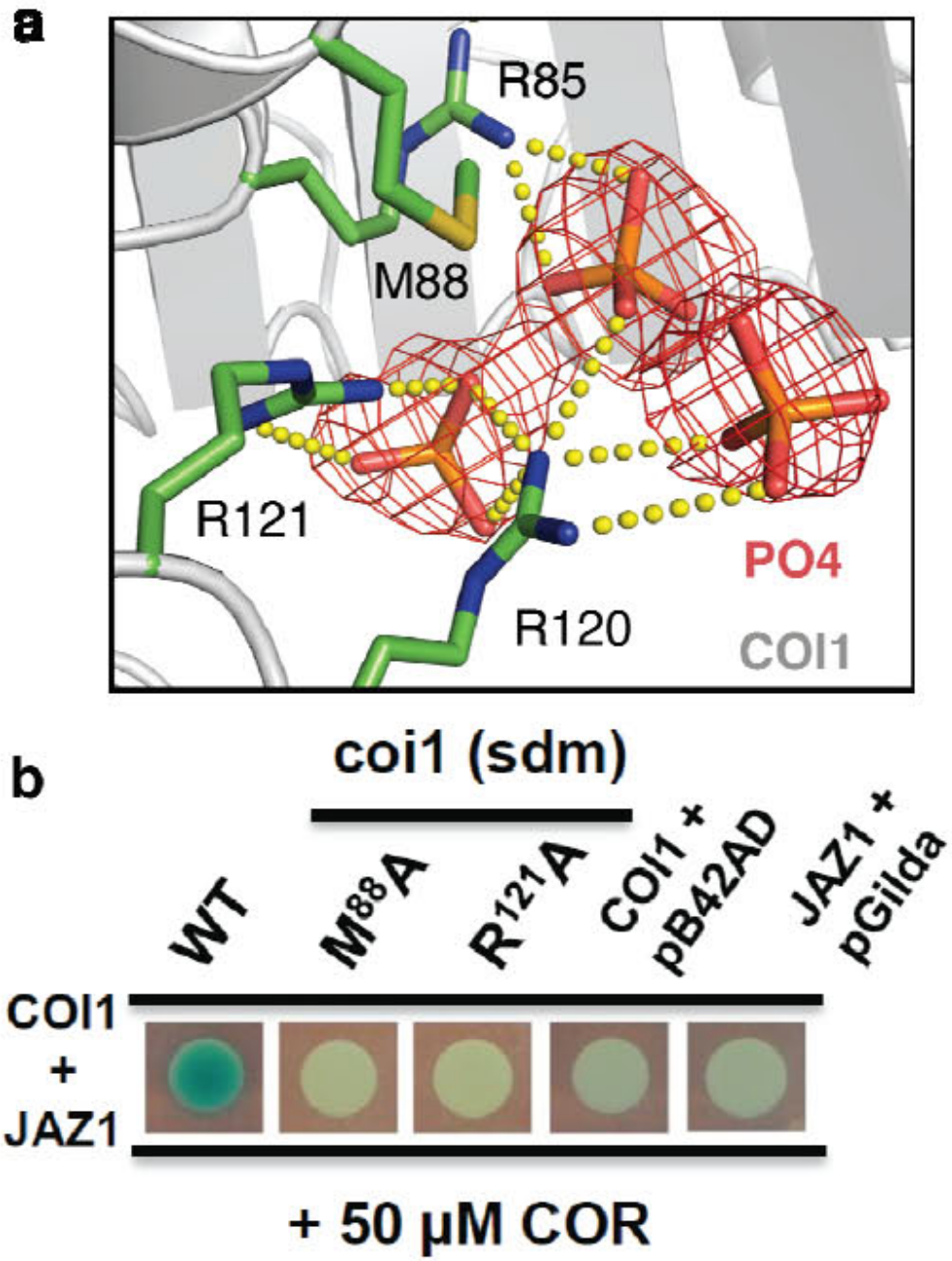
a
R85
M88
R121
R120
PO4
COI1
b
coi1 (sdm)
WT
M88A
R121A
COI1 + pB42AD
JAZ1 + pGilda
COI1 + JAZ1
+ 50 µM COR

Figure 6.2 Mutational studies of COI1 residues in the putative $InsP_5$ binding site. a. Close-up view of COI1 residues (green stick) in close vicinity to the inorganic phosphates occupying the $InsP_5$ binding pocket (orange stick, with along with positive F_o-F_c density in red mesh). Hydrogen bonds are shown with yellow dashes. b. Interaction of wild-type COI1 and COI1 mutants with JAZ1 detected by yeast two-hybrid assay. The term "sdm" indicates site-directed mutations.

6.2 Materials and Methods

6.2a Site-directed mutagenesis.

Individual amino acid residues in the LRR domain of COI1 proteins were mutated to alanine using the Quick-Change II site-directed mutagenesis kit (Stratagene). Mutant proteins were co-expressed with JAZ1 (JAZ1:pB42AD) in yeast to detect protein-protein interactions.

6.2b Yeast two-hybrid (Y2H) assay.

The coding sequences (CDS) of the *Arabidopsis thaliana* gene *COI1* (At2g39940) and *coi1* site-directed mutants were cloned into the Y2H bait vector pGILDA (Clontech) using XmaI and XhoI restriction enzyme recognition sequences previously added to the 5' and 3' end of the *COI1* CDS, respectively, creating DNA-binding domain (LexA:COI1 and LexA:*coi1*) protein fusions. The CDS of *Arabidopsis thaliana JAZ1* gene (At1g19180) was cloned into the Y2H prey vector pB42AD (Clontech) creating a transcriptional activation domain (AD:JAZ1) fusion protein. Individual wild-type and mutant *COI1* constructs were co-transformed with *JAZ1* constructs into *Saccharomyces cerevisae* strain EGY48 (p8opLacZ) using the frozen-EZ yeast transformation II kit (Zymo Research). Transformants were selected on SD-glucose medium (BD Biosciences) supplemented with –Ura/-Trp/–His drop-out solution (BD Biosciences). To detect the interaction between COI1 and JAZ1, transformants that had been selected in SD-Glu medium were resuspended in sterile water.

Ten µl of each suspension was spotted onto inducing media (SD-Galactose/Raffinose –UWH; BD Biosciences) supplemented with 80 µg mL^{-1} X-Gal and 50 µM coronatine (Sigma). Y2H assays plates were incubated in the dark at 20°C and photographed 7 days later. Induced yeast cells were analyzed for COI1 and JAZ1 expression levels by western blotting using epitope-specific antibodies (data not shown).

6.2c Inositol phosphate reconstitution assays.

COI1-ASK1 complex was separated from pre-bound inositol phosphate by dialysis. Briefly, proteins were mixed with 10% glycerol and incubated in 2 M ammonium phosphate, 100 mM Bis-Tris propane pH=7.0, 200 mM NaCl, 10% glycerol, at 4°C for >24hrs with a minimum of 3x buffer changes at 100x sample volume. Samples were then transferred to 20 mM Tris-HCl, pH=8.0, 200 mM NaCl, 10% glycerol, at 4°C for >24hrs with a minimum of 3 buffer changes at 100x sample volume. Inositol phosphate rescue experiments were conducted according to the radioligand binding assays described above in the presence of 300 nM ^{3}H-coronatine with nonspecific binding determined in the presence of 300 mM coronatine.

6.2d Mass spectrometry analysis of inositol phosphate purified from COI1-ASK1.

MS experiments were conducted on a Finnigan (San Jose, CA) LTQ linear ion-trap mass spectrometer (ITMS) with Xcalibur operating system. Methanol was continuously infused (10 mL min^{-1}) to the ESI source, where the skimmer

was set at ground potential, the electrospray needle was set at 4.5 kV, and the temperature of the heated capillary was 275°C. The sample was diluted with equal volume of 2% ammonia in methanol and 10 ml was flow injected. The automatic gain control of the ion trap was set at $2x10^4$, with a maximum injection time of 50 ms. Helium was used as the buffer and collision gas at a pressure of $1x10^{-3}$ mbar (0.75 mTorr). The MS^n (n=2,3,4,5) experiments were carried out with an optimized relative collision energy ranging from 12–16% with an activation q value at 0.25. The activation time was set at 30–60 ms. The mass spectra were acquired in the profile mode and were accumulated for 3–5 min for MS^n-spectra. The mass resolution of the instrument was tuned to 0.6 Da at half peak height.

CHAPTER 7

Discussions

Our structural and pharmacological analyses reveal not only the essential components of the receptor system, but also the detailed mechanism by which these components cooperatively assemble and recognize the hormonal signal through a network of interactions. Our data identify the true JA receptor as a three-molecule co-receptor complex, consisting of COI1, JAZ degron, and inositol pentakisphosphate, all of which are indispensable for high affinity hormone binding. Our analyses also define the JAZ degron boundaries as a unique bi-partite sequence that binds COI1 and directly participates in hormone recognition. Unexpectedly, the N-terminal clamp region of the JAZ1 degron that is critical for hormone binding is diverse amongst JAZ proteins. This variable sequence might create a family of COI1-JAZ co-receptors that respond differentially to the hormone.

The crystal structure of the COI1-JAZ1 co-receptor in complex with JA-Ile revealed a drastically different binding mode of the hormone as predicted by computational modeling (Yan et al., 2009). Although COI1 shares high sequence homology with TIR1, subtle structural differences and the integration of two additional factors critical for ligand binding give rise to a hormone-binding pocket in COI1 that is challenging to model. For the same reason, the structural nature of the ligand-free form of the F-box protein cannot be modeled with accuracy. The direct interactions of the hormone with both COI1 and the

JAZ protein as observed in the crystal, nonetheless, support a molecular glue mechanism previously proposed for the auxin system (Tan et al., 2007).

Discovery of the inositol pentakisphosphate cofactor of COI1 offers profound implications for the role of inositol phosphates in plant hormone signaling. COI1 co-purifies with a single isoform of $InsP_5$, $Ins(1,2,4,5,6)P_5$, indicating selectivity at the receptor level. However, both inositol (1,2,4,5,6) pentakisphosphate and inositol (1,4,5,6) tetrakisphosphate support high affinity hormone binding in our reconstitution assays, leaving the identity of the physiologically relevant form of inositol phosphate an open question.

Lastly, our study is the latest in a series of receptor structures for plant hormones, including auxin (Tan et al., 2007), gibberellin (Murase et al., 2008; Shimada et al., 2008), and abscisic acid (Melcher et al., 2009; Miyazono et al., 2009; Nishimura et al., 2009; Santiago et al., 2009; Yin et al., 2009). Despite different structural mechanisms, a common theme of hormone-mediated protein interactions emerges as a unique strategy favored by plant systems throughout evolution.

Curriculum Vitae

Laura B. Sheard

Personal:

Birth Date: May 14, 1985
Birthplace: Allentown Pennsylvania USA

Academic Background/Education:

Year Degree, Department, University, City, State

2012 Ph.D. in Pharmacology, expected. University of Washington, Seattle, WA

2007 B.S. in Neuroscience. Muhlenberg College, Allentown, PA

Research and Professional Experience:

Ph.D Research in Pharmacology, 2007-2012
Department of Pharmacology, University of Washington
Dr. Ning Zheng (nzheng@uw.edu)
Structural and pharmacological study of ubiquitin ligases as plant hormone receptors for auxin, jasmonate, and strigolactone.

Merck and Co. Intern in Basic Research, 2007
Department of Stroke and Neurodegeneration

Honors Research in Neuroscience, 2004-2007
Department of Biology, Muhlenberg College
Investigation of key domains in the recognition of allopregnanolone on the $GABA_A$ receptor

MIT Intern in Biochemistry, 2006
Department of Chemistry, Massachusetts Institute of Technology
Characterization of biotin ligase system for use in detecting protein-protein interactions.

Field Study—Medicinal Plant Use in Las Juntas de Abangares, Costa Rica, 2005
Department of Biology, Muhlenberg College

Honors, Awards, and Fellowships:

2011-12 Graduate Fellowship, USDA National Institute for Food and Agriculture (NIFA)

2011 Competitive Travel Award, International Conference in Arabidopsis Research
(NSF)

2009-10 Graduate Fellowship, National Institute of Health (NIH) UW CMB Training Grant

2007 Honors in Neuroscience, Muhlenberg College

2007 Phi Beta Kappa National Honor Society

2007 Finalist, Fulbright Foundation Scholar

2006 Competitive Summer Study Award, Honors Research, Muhlenberg College

2006 Competitive Travel Award, Field Work in Costa Rica, Muhlenberg College

2005 Barry M. Goldwater National Undergraduate Science and Engineering Award

Publications (published/in press):

Sheard, LB and Zheng N. Plant Biology: Signal advance for abscisic acid. ***Nature*** (2009) vol. 462 (7273) pp 575-6 (News & Views)

Sheard, LB, Tan X, Mao H, Withers J, Ben-Nissan G, Hinds TR, Kobayashi Y, Hsu F, Sharon M, Browse J, He SY, Rizo J, Howe GA, and Zheng N. Jasmonate perception by inositol phosphate-potentiated COI1-JAZ co-receptor. ***Nature*** 2010 vol. 468 (7322) pp 400-5

Other Publications (submitted/in preparation)

Calderón Villalobos LIA, Lee S, De Oliveira C, Ivetac A, Brandt W, Armitage L, **Sheard LB**, Tan X, Parry G, Mao H, McCammonn JA, Zheng N, Napier R, Kepinski S, Estelle M. TIR1/AFBs and Aux/IAAs constitute a combinatorial co-receptor system to perceive auxin with differential sensitivities. ***Nature Chemical Biology*** (manuscript under review)

Shyu C, Figueroa P, DePewa C, Cooke TF, **Sheard LB**, Katsir L, Zheng N, Browse J, Howe GA. JAZ8 Lacks a Canonical Jasmonate Degron and has an EAR Motif that Mediates Transcriptional Repression of Jasmonate Responses in Arabidopsis. ***Plant Cell*** (manuscript under review)

Presentation/Abstracts:

Invited Speaker:
Plant Defense in 3D: Structural & pharmacological insight into jasmonate perception. ***SAMPL (Seattle Area Model Plant Labs) Lecture Series***. Seattle, WA, January 2011

An F-box receptor for jasmonates: pharmacological and crystallographic studies. ***2010 Arabidopsis Meeting*** San Diego CA, December 2010

Poster Presentation:
Jasmonate perception by inositol phosphate-potentiated COI1-JAZ co-receptor. ***Howard Hughes Medical Institute (HHMI) Investigator Meeting***, Janelia Farms, September 2010

Jasmonate perception by inositol phosphate-potentiated COI1-JAZ co-receptor. ***2011 International Conference in Arabidopsis Research***, Madison WI, June 2011

Patents

Sheard LB and N Zheng. *Methods and Compositions for Targeted Protein Degradation.* PCT Patent Appl. No. PCT/US2011/039676. Filed June 8 2011.

References

Adams, P.D., Grosse-Kunstleve, R.W., Hung, L.W., Ioerger, T.R., McCoy, A.J., Moriarty, N.W., Read, R.J., Sacchettini, J.C., Sauter, N.K., and Terwilliger, T.C. (2002). PHENIX: building new software for automated crystallographic structure determination. Acta Crystallogr D Biol Crystallogr *58*, 1948-1954.

Akiyama, K., Matsuzaki, K., and Hayashi, H. (2005). Plant sesquiterpenes induce hyphal branching in arbuscular mycorrhizal fungi. Nature *435*, 824-827.

Bouwmeester, H.J., Matusova, R., Zhongkui, S., and Beale, M.H. (2003). Secondary metabolite signalling in host-parasitic plant interactions. Curr Opin Plant Biol *6*, 358-364.

Browse, J. (2009). Jasmonate passes muster: a receptor and targets for the defense hormone. Annu Rev Plant Biol *60*, 183-205.

Brünger, A.T., Adams, P.D., Clore, G.M., DeLano, W.L., Gros, P., Grosse-Kunstleve, R.W., Jiang, J.S., Kuszewski, J., Nilges, M., Pannu, N.S.*, et al.* (1998). Crystallography & NMR system: A new software suite for macromolecular structure determination. Acta Crystallogr D Biol Crystallogr *54*, 905-921.

Cheng, Y., and Prusoff, W.H. (1973). Relationship between the inhibition constant (K1) and the concentration of inhibitor which causes 50 per cent inhibition (I50) of an enzymatic reaction. Biochem Pharmacol *22*, 3099-3108.

Chini, A., Fonseca, S., Fernández, G., Adie, B., Chico, J.M., Lorenzo, O., García-Casado, G., López-Vidriero, I., Lozano, F.M., Ponce, M.R.*, et al.* (2007). The JAZ family of repressors is the missing link in jasmonate signalling. Nature *448*, 666-671.

Chung, H.S., Cooke, T.F., Depew, C.L., Patel, L.C., Ogawa, N., Kobayashi, Y., and Howe, G.A. (2010). Alternative splicing expands the repertoire of dominant JAZ repressors of jasmonate signaling. Plant J *63*, 613-622.

Chung, H.S., and Howe, G.A. (2009). A critical role for the TIFY motif in repression of jasmonate signaling by a stabilized splice variant of the JASMONATE ZIM-domain protein JAZ10 in Arabidopsis. Plant Cell *21*, 131-145.

Delaglio, F., Grzesiek, S., Vuister, G.W., Zhu, G., Pfeifer, J., and Bax, A. (1995). NMRPipe: a multidimensional spectral processing system based on UNIX pipes. J Biomol NMR *6*, 277-293.

Dharmasiri, N., Dharmasiri, S., and Estelle, M. (2005). The F-box protein TIR1 is an auxin receptor. Nature *435*, 441-445.

Dharmasiri, N., and Estelle, M. (2004). Auxin signaling and regulated protein degradation. Trends Plant Sci *9*, 302-308.

Domagalska, M.A., and Leyser, O. (2011). Signal integration in the control of shoot branching. Nat Rev Mol Cell Biol *12*, 211-221.

Feys, B., Benedetti, C.E., Penfold, C.N., and Turner, J.G. (1994). Arabidopsis Mutants Selected for Resistance to the Phytotoxin Coronatine Are Male Sterile, Insensitive to Methyl Jasmonate, and Resistant to a Bacterial Pathogen. Plant Cell *6*, 751-759.

Fonseca, S., Chico, J.M., and Solano, R. (2009). The jasmonate pathway: the ligand, the receptor and the core signalling module. Curr Opin Plant Biol *12*, 539-547.

Fujii, H., Chinnusamy, V., Rodrigues, A., Rubio, S., Antoni, R., Park, S.Y., Cutler, S.R., Sheen, J., Rodriguez, P.L., and Zhu, J.K. (2009). In vitro reconstitution of an abscisic acid signalling pathway. Nature *462*, 660-664.

Gray, W.M., del Pozo, J.C., Walker, L., Hobbie, L., Risseeuw, E., Banks, T., Crosby, W.L., Yang, M., Ma, H., and Estelle, M. (1999). Identification of an SCF ubiquitin-ligase complex required for auxin response in Arabidopsis thaliana. Genes Dev *13*, 1678-1691.

Gray, W.M., Kepinski, S., Rouse, D., Leyser, O., and Estelle, M. (2001). Auxin regulates SCF(TIR1)-dependent degradation of AUX/IAA proteins. Nature *414*, 271-276.

Grunewald, W., Vanholme, B., Pauwels, L., Plovie, E., Inzé, D., Gheysen, G., and Goossens, A. (2009). Expression of the Arabidopsis jasmonate signalling repressor JAZ1/TIFY10A is stimulated by auxin. EMBO Rep *10*, 923-928.

Henderson, J., Bauly, J.M., Ashford, D.A., Oliver, S.C., Hawes, C.R., Lazarus, C.M., Venis, M.A., and Napier, R.M. (1997). Retention of maize auxin-binding

protein in the endoplasmic reticulum: quantifying escape and the role of auxin. Planta *202*, 313-323.

Johnson, B.A. (2004). Using NMRView to visualize and analyze the NMR spectra of macromolecules. Methods Mol Biol *278*, 313-352.

Jones, T.A., Zou, J.Y., Cowan, S.W., and Kjeldgaard, M. (1991). Improved methods for building protein models in electron density maps and the location of errors in these models. Acta Crystallogr A *47 (Pt 2)*, 110-119.

Katsir, L., Schilmiller, A.L., Staswick, P.E., He, S.Y., and Howe, G.A. (2008). COI1 is a critical component of a receptor for jasmonate and the bacterial virulence factor coronatine. Proc Natl Acad Sci U S A *105*, 7100-7105.

Kepinski, S., and Leyser, O. (2005). The Arabidopsis F-box protein TIR1 is an auxin receptor. Nature *435*, 446-451.

Koo, A.J., Gao, X., Jones, A.D., and Howe, G.A. (2009). A rapid wound signal activates the systemic synthesis of bioactive jasmonates in Arabidopsis. Plant J *59*, 974-986.

Liscum, E., and Reed, J.W. (2002). Genetics of Aux/IAA and ARF action in plant growth and development. Plant Mol Biol *49*, 387-400.

Lorenzo, O., Chico, J.M., Sánchez-Serrano, J.J., and Solano, R. (2004). JASMONATE-INSENSITIVE1 encodes a MYC transcription factor essential to discriminate between different jasmonate-regulated defense responses in Arabidopsis. Plant Cell *16*, 1938-1950.

Ma, Y., Szostkiewicz, I., Korte, A., Moes, D., Yang, Y., Christmann, A., and Grill, E. (2009). Regulators of PP2C phosphatase activity function as abscisic acid sensors. Science *324*, 1064-1068.

Melcher, K., Ng, L.M., Zhou, X.E., Soon, F.F., Xu, Y., Suino-Powell, K.M., Park, S.Y., Weiner, J.J., Fujii, H., Chinnusamy, V.*, et al.* (2009). A gate-latch-lock mechanism for hormone signalling by abscisic acid receptors. Nature *462*, 602-608.

Melotto, M., Mecey, C., Niu, Y., Chung, H.S., Katsir, L., Yao, J., Zeng, W., Thines, B., Staswick, P., Browse, J.*, et al.* (2008). A critical role of two positively charged amino acids in the Jas motif of Arabidopsis JAZ proteins in mediating

coronatine- and jasmonoyl isoleucine-dependent interactions with the COI1 F-box protein. Plant J *55*, 979-988.

Miyazono, K., Miyakawa, T., Sawano, Y., Kubota, K., Kang, H.J., Asano, A., Miyauchi, Y., Takahashi, M., Zhi, Y., Fujita, Y.*, et al.* (2009). Structural basis of abscisic acid signalling. Nature *462*, 609-614.

Murase, K., Hirano, Y., Sun, T.P., and Hakoshima, T. (2008). Gibberellin-induced DELLA recognition by the gibberellin receptor GID1. Nature *456*, 459-463.

Nettleton, E.J., Sunde, M., Lai, Z., Kelly, J.W., Dobson, C.M., and Robinson, C.V. (1998). Protein subunit interactions and structural integrity of amyloidogenic transthyretins: evidence from electrospray mass spectrometry. J Mol Biol *281*, 553-564.

Nishimura, N., Hitomi, K., Arvai, A.S., Rambo, R.P., Hitomi, C., Cutler, S.R., Schroeder, J.I., and Getzoff, E.D. (2009). Structural mechanism of abscisic acid binding and signaling by dimeric PYR1. Science *326*, 1373-1379.

Ogawa, N., and Kobayashi, Y. (2011). Synthesis of the amino acid conjugates of epi-jasmonic acid. Amino Acids.

Park, S.Y., Fung, P., Nishimura, N., Jensen, D.R., Fujii, H., Zhao, Y., Lumba, S., Santiago, J., Rodrigues, A., Chow, T.F.*, et al.* (2009). Abscisic acid inhibits type 2C protein phosphatases via the PYR/PYL family of START proteins. Science *324*, 1068-1071.

Sadrzadeh, S.M., Vincenzi, F.F., and Hinds, T.R. (1993). Simultaneous measurement of multiple membrane ATPases in microtiter plates. J Pharmacol Toxicol Methods *30*, 103-110.

Santiago, J., Dupeux, F., Round, A., Antoni, R., Park, S.Y., Jamin, M., Cutler, S.R., Rodriguez, P.L., and Márquez, J.A. (2009). The abscisic acid receptor PYR1 in complex with abscisic acid. Nature *462*, 665-668.

Shimada, A., Ueguchi-Tanaka, M., Nakatsu, T., Nakajima, M., Naoe, Y., Ohmiya, H., Kato, H., and Matsuoka, M. (2008). Structural basis for gibberellin recognition by its receptor GID1. Nature *456*, 520-523.

Staswick, P.E., and Tiryaki, I. (2004). The oxylipin signal jasmonic acid is activated by an enzyme that conjugates it to isoleucine in Arabidopsis. Plant Cell *16*, 2117-2127.

Stephens, L.R., Hawkins, P.T., Stanley, A.F., Moore, T., Poyner, D.R., Morris, P.J., Hanley, M.R., Kay, R.R., and Irvine, R.F. (1991). myo-inositol pentakisphosphates. Structure, biological occurrence and phosphorylation to myo-inositol hexakisphosphate. Biochem J *275 (Pt 2)*, 485-499.

Suza, W.P., and Staswick, P.E. (2008). The role of JAR1 in Jasmonoyl-L: -isoleucine production during Arabidopsis wound response. Planta *227*, 1221-1232.

Tan, X., Calderon-Villalobos, L.I., Sharon, M., Zheng, C., Robinson, C.V., Estelle, M., and Zheng, N. (2007). Mechanism of auxin perception by the TIR1 ubiquitin ligase. Nature *446*, 640-645.

Thines, B., Katsir, L., Melotto, M., Niu, Y., Mandaokar, A., Liu, G., Nomura, K., He, S.Y., Howe, G.A., and Browse, J. (2007). JAZ repressor proteins are targets of the SCF(COI1) complex during jasmonate signalling. Nature *448*, 661-665.

Ulmasov, T., Hagen, G., and Guilfoyle, T.J. (1997). ARF1, a transcription factor that binds to auxin response elements. Science *276*, 1865-1868.

Ulmasov, T., Liu, Z.B., Hagen, G., and Guilfoyle, T.J. (1995). Composite structure of auxin response elements. Plant Cell *7*, 1611-1623.

Woodward, A.W., and Bartel, B. (2005). Auxin: regulation, action, and interaction. Ann Bot *95*, 707-735.

Xie, D.X., Feys, B.F., James, S., Nieto-Rostro, M., and Turner, J.G. (1998). COI1: an Arabidopsis gene required for jasmonate-regulated defense and fertility. Science *280*, 1091-1094.

Yan, J., Zhang, C., Gu, M., Bai, Z., Zhang, W., Qi, T., Cheng, Z., Peng, W., Luo, H., Nan, F.*, et al.* (2009). The Arabidopsis CORONATINE INSENSITIVE1 protein is a jasmonate receptor. Plant Cell *21*, 2220-2236.

Yan, Y., Stolz, S., Chételat, A., Reymond, P., Pagni, M., Dubugnon, L., and Farmer, E.E. (2007). A downstream mediator in the growth repression limb of the jasmonate pathway. Plant Cell *19*, 2470-2483.

Yin, P., Fan, H., Hao, Q., Yuan, X., Wu, D., Pang, Y., Yan, C., Li, W., Wang, J., and Yan, N. (2009). Structural insights into the mechanism of abscisic acid signaling by PYL proteins. Nat Struct Mol Biol *16*, 1230-1236.